VARIATIONAL CALCULATIONS

OF

LAMBDA BINDING ENERGIES IN HYPERNUCLEI

by

TZE-CHIEN HAZEL HO, M.Sc.

A Thesis

Submitted to the Faculty of Graduate Studies
in Partial Fulfilment of the Requirements

for the Degree

Doctor of Philosophy

McMaster University

October 1969

LAMBDA BINDING ENERGIES IN HYPERNUCLEI

DOCTOR OF PHILOSOPHY (1969) McMASTER UNIVERSITY
(Physics) Hamilton, Ontario.

TITLE: Variational Calculations of Lambda Binding Energies in Hypernuclei

AUTHOR: Tze-Chien Hazel Ho, B.Sc. (University of Hong Kong)
M.Sc. (University of Waterloo)

SUPERVISOR: Professor A. B. Volkov

NUMBER OF PAGES: vi, 114

SCOPE AND CONTENTS:

Variational calculations for hypernuclei and their corresponding nuclear cores have been performed with phenomenological effective Λ-N and N-N interactions. Effects of deformation and Majorana exchange on the Λ binding energies have been studied. The influence of density dependence in both the Λ-N and N-N force has been investigated. The three-body ΛNN interaction has also been considered qualitatively. All these effects help to reduce the Λ binding energies in hypernuclei.

In addition to the variational calculations, the rigid alpha model has been used to determine the Λ binding energy in ${}^{5}_{\Lambda}\mathrm{He}$. A comparison of the methods is given.

Finally, excited states of some hypernuclei have been calculated using the variational ground state equilibrium size.

ACKNOWLEDGEMENTS

I am deeply grateful to Professor A.B. Volkov for his giving me a thorough introduction to the study of nuclear physics, and his patient and encouraging advice which has made this work possible.

My great gratitude goes to Dr. Y. Nogami and Dr. R.K. Bhaduri for the instructive discussions and valuable information in the field of hypernuclear physics.

I also would like to thank Mr. D. Hughes and Dr. M. Manning for allowing me to use their computer programs without which the computations would be much more difficult. To the staff of the Computer Centre, McMaster University, I would like to express my appreciation for the help they have given me.

I am obliged to both the University Women's Club of Hamilton for the Jean Gall Memorial Scholarship (1967-1968) and the McMaster University for financial support.

Finally, I would like to thank Mrs. H. Kennelly whose cheerful and efficient typing of this thesis is very much appreciated.

TABLE OF CONTENTS

LIST OF TABLES

CHAPTER 1

INTRODUCTION

Hypernuclei are stable bound states of the Λ hyperon with various nuclei. The first specimen was discovered by Danysz and Pniewski[1/] in a photographic emulsion. The hypernucleus was formed by a cosmic ray particle collision with a nucleus in the emulsion. Now hypernuclei are produced by bombarding nuclei with pions or K^- mesons.

The standard notation for hypernuclei is ${}^{A+1}_{\Lambda}X$ where ${}^{A}X$ is the nucleus core to which the Λ particle is bound.

The interpretation of these systems as stable states is supported by two facts: the hypernuclei half lives are about equal to the lambda particle half life, and the energy released in a pionic hypernuclear decay is about equal to that for free lambda decay (37.5 MeV). The observed energy differences going up to more than 10 MeV is largely the Λ particle binding energy in the hypernucleus.

The Λ particle half life is of the order of 10^{-10} second. The time required to traverse a typical mean free path in liquid hydrogen is considerably greater than the half life and consequently, a study of the lambda-nucleon (Λ-N) interaction from direct collisions is difficult. The most

detailed information about the interaction was for some time deduced only from the binding energies of the hypernuclei.

A compilation of the binding energies of light hypernuclei (A<16),measured by the European K^- Collaboration and the EFINS-Northwestern Collaboration up to 1966, was made by Gajewski et al[2]. A more recent experiment in the K^- collaboration[3] yields slightly different results. These observed binding energies are listed in Table 1. The results are affected by an error of about 0.05 MeV,which is not included in the table, due to uncertainty in the determination of the emulsion density.

Over the past few years measurements of the Λ-p cross section have been made from low energy scattering events following hyperon production in bubble chambers[4-8,10-12]. The general behaviour of the Λ-p elastic cross section as function of CM energy is shown in Fig. 3. The most detailed results have been reported by the Maryland group and by the Rehavoth Heidelberg group.

Differential cross-section information is absent in most experiments due to the poor statistics. One experiment[8] has indicated a predominantly backward scattering of the Λ particle. However, some experiments seem to favour a forward scattering, while the rest have reported an isotropic angular distribution.

TABLE 1

Experimental Λ binding energies in MeV

	Gajewski et al compilation Ref. 2	K^- collaboration new result Ref. 3
${}^{3}_{\Lambda}H$	0.20 ± 0.12	-0.08 ± 0.08
${}^{4}_{\Lambda}H \rightarrow \pi^- {}^{4}He$	2.26 ± 0.07	2.11 ± 0.04
Others	1.86 ± 0.01	1.95 ± 0.06
${}^{4}_{\Lambda}He$	2.20 ± 0.06	2.20 ± 0.04
${}^{5}_{\Lambda}He$	3.08 ± 0.03	2.96 ± 0.02
${}^{6}_{\Lambda}He$	4.09 ± 0.27	4.25 ± 0.21
${}^{7}_{\Lambda}He$	4.67 ± 0.28	4.54 ± 0.12
${}^{7}_{\Lambda}Li$	5.46 ± 0.12	5.44 ± 0.08
${}^{7}_{\Lambda}Be$	5.39 ± 0.24	4.91 ± 0.19
${}^{8}_{\Lambda}Li$	6.72 ± 0.08	6.69 ± 0.07
${}^{8}_{\Lambda}Be$	6.67 ± 0.16	6.86 ± 0.09
${}^{9}_{\Lambda}Li$	8.27 ± 0.18	7.97 ± 0.25
${}^{9}_{\Lambda}Be \rightarrow \pi^- {}^{4}B_{gs}$	6.68 ± 0.09	6.45 ± 0.06
Others	6.61 ± 0.17	6.15 ± 0.13
${}^{11}_{\Lambda}B$	10.30 ± 0.14	-
${}^{12}_{\Lambda}B$	11.26 ± 0.16	10.81 ± 0.16
${}^{13}_{\Lambda}C$	10.51 ± 0.51	-

Phenomenological potentials have been derived to reproduce the scattering parameters. However, a serious discrepancy appears when these potentials are applied to the bound systems, since as yet every potential obtained from the two-body data overbinds some hypernuclei in conventional binding energy calculations.

In this thesis a number of effects are examined which help to reduce the discrepancy between the calculated and observed binding energies. In order to obtain meaningful Λ particle binding energies in hypernuclei it is rather important to have a good, self-consistent description of the nuclear core. Therefore, it is necessary to examine the nature of the N-N force as well as the Λ-N force, and it is also necessary to examine and reproduce the pertinent properties of the nuclei relevant to hypernuclei studies. Thus, in the following chapters, descriptions of the hypernucleus and its core nucleus are presented side by side; and the effects of an appropriate nuclear structure and a correct choice of a N-N force on the Λ binding energy will be discussed.

In Chapter 2, a general theoretical discussion of the variational method is given which is applicable to both the nucleus and the hypernucleus as well. Variational considerations require a deformed representation of states in order to

adequately describe the lp shell hypernuclei and nuclei. Chapter 3 deals with both the phenomenological Λ-N and N-N potentials. The G matrix approach to nuclear matter suggests a relatively simple density dependent central effective N-N potential. The phenomenological N-N potential has been taken as a guide for constructing a Λ-N potential. The Λ-N and N-N potentials are then used, in Chapter 4, to calculate the properties of the ${}^{5}_{\Lambda}$He hypernucleus as well as the α particle core. The size, binding energy and spectrum of ^{4}He are taken as part of the criteria for determining an N-N force which is then used in the lp-shell nuclei and hypernuclei calculations. Several approaches have been employed to calculate the binding energy of ${}^{5}_{\Lambda}$He including the effect of a density dependence in the Λ-N force. Chapter 5 contains a study of the lp-shell hypernuclei binding energies. The influence on the Λ binding energies of deformation, a Λ-N space-exchange potential, density dependence in the N-N and the Λ-N force are investigated. Chapter 6 investigates some interesting hypernuclear excited states, in particular the isomeric states of ${}^{7}_{\Lambda}$He . Some of the electromagnetic radiation transition rates have been calculated. Chapter 7 is concerned with the effects of a ΛNN three-body interaction. Variational calculations of the Λ binding energies are performed using a phenomenological ΛNN force for the p-shell hypernuclei, and the rigid α model is used in the case of ${}^{5}_{\Lambda}$He.

CHAPTER 2

THE VARIATIONAL CALCULATION AND THE "DEFORMED" REPRESENTATION

The nuclear shell model, which was first proposed to explain certain experimental phenomena such as the magic numbers, ground state spins, etc., can be considered as an approximate representation of the nuclear many-body system.

The Hamiltonian of the A-particle system

$$H = \sum_{i=1}^{A} T_i - T_{cm} + \sum_{i<j} v_{ij}(\underset{\sim}{r}_{ij}), \qquad (2.1)$$

where T_i is the kinetic energy of the single particle i,

T_{cm} is the kinetic energy of the centre-of-mass,

and $v_{ij}(\underset{\sim}{r}_{ij})$ is the two-body potential depending on the relative co-ordinates $\underset{\sim}{r}_{ij} = \underset{\sim}{r}_i - \underset{\sim}{r}_j$, representing the intrinsic energy of the system.

Since no exact solution for more than two interacting bodies exists, approximate solutions have had to be developed. One of the basic principles in physics is the variational principle which states that in a function space F, the solutions of the physical equation being studied are some functions ψ of F for which a functional $Q(\psi)$ is stationary, i.e. the physical equation is equivalent to the variational equation

$$\delta Q(\psi) = 0. \qquad (2.3)$$

The equation to be solved here is the Schroedinger equation

$$H\psi = E\psi \qquad (2.3)$$

We can use a soluble system of Hamiltonian H_o such that

$$H_o\psi_n = E_n\psi_n \qquad (2.4)$$

where $\psi_n = \psi_n(r_1, r_2, \ldots, r_A)$ and $E_n \leq E_{n+1}$. $\{\psi_n\}$ is a complete orthonormal set of wave vectors in the Hilbert space F_o. Any solution ψ of (2.3) can be expressed as

$$\psi = \sum_{n=1}^{\infty} c_n \psi_n \quad \text{with} \quad \sum_{n=1}^{\infty} |c_n|^2 = 1.$$

The average energy in the state ψ is given by

$$\bar{E} = \langle\psi|H|\psi\rangle .$$

The appropriate variational equation to be solved is

$$\delta\bar{E} = 0, \quad \text{subject to the condition } \int \psi^*\psi d\tau = 1,$$

i.e. $$\delta\bar{E} = \delta[\int\psi^*H\psi d\tau / \int\psi^*\psi d\tau] = 0.$$

The variation in $\bar{E}$ is brought about by varying ψ and ψ^* independently

$$\psi \to \psi+\delta\psi \quad \text{and} \quad \psi^* \to \psi^* + \delta\psi^*$$

$$\delta\bar{E} = \int\delta\psi^*H\psi d\tau / \int\psi^*\psi d\tau - \int\psi^*H\psi d\tau \int\delta\psi^*\psi d\tau / (\int\psi^*\psi d\tau)^2 +$$

$$\text{complex conjugate} = 0.$$

which, on ignoring second order terms, gives

$$\int \delta\psi^* (H-\lambda)\psi d\tau = 0,$$

and
$$\int \psi^* (H-\lambda)\delta\psi d\tau = 0, \qquad (2.5)$$

where
$$\lambda = \int \psi^* H \psi d\tau / \int \psi^* \psi d\tau.$$

(2.5), when written as $(H-\lambda)\psi = 0$, is simply equation (2.3).

In order to solve (2.5) we let

$$\delta\psi = \sum_{n=1}^{\infty} d_n \psi_n, \text{ and}$$

$$\psi + \delta\psi = \sum_{n=1}^{\infty} (d_n + C_n)\psi_n.$$

Substituting the above expression into the integrand of (2.5) yields

$$\sum_m \sum_n d_m C_n \langle \psi_m | H-\lambda | \psi_n \rangle = 0.$$

Since the d_m are arbitrary,

$$\sum_{n=1}^{\infty} C_n \langle \psi_m | H-\lambda | \psi_n \rangle = 0. \qquad (2.6)$$

The exact solution of (2.6) is impossible in the infinite space, and the Ritz variational method consists of seeking solutions of (2.3) among the functions of a truncated subspace F' of dimension N. (2.5) is thus approximated by

$$\sum_{n=1}^{N} C_n \langle \psi_m | H-\lambda | \psi_n \rangle = 0,$$

or
$$\sum_{n=1}^{N} C_n (H_{mn} - \lambda \delta_{mn}) = 0, \qquad (2.7)$$

where $H_{mn} = \int \psi_m^* H \psi_n \, d\tau$, $\delta_{mn} = \begin{cases} 1 \text{ if } m=n \\ 0 \text{ otherwise} \end{cases}$

(2.7) is a set of homogeneous equations which are soluble if and only if

$$\det |H_{mn} - \lambda \delta_{mn}| = 0.$$

Consequently the possible values of λ can be found by diagonalization of the matrix (H_{mn}). This is, in fact, the shell model calculation, where the ψ_m are appropriate product functions of the spherical harmonic oscillator.

The nucleons, being identical particles, obey the Pauli exclusion principle, and hence the wave function should be antisymmetrized with respect to the exchange of any pair of the co-ordinates. Generally, such a wave function is expressed as a Slater determinant,

$$\hat{A}\psi = \sum_P (-1)^P P \prod_{i=1}^{A} \phi_{\alpha_i}(r_i) \qquad (2.8)$$

where P is the permutation operator acting on the product wave function. ϕ_{α_i} is taken to be the harmonic oscillator single particle wave function which is believed to be a good approximation to the 'best' set of single particle wave functions given by the Hartree-Fock variational solution. The use of Hartree-Fock single particle states should result in better results with a truncated representation.

The shell-model calculation used in this thesis has

two special features which we shall now describe.

The usual shell model approximation assumes that the A-n particles filling up the major shells form a core with the n "valence" particles occupying levels in the unfilled shell. The conventional prescription is to calculate the interaction of the "valence" particles and use "experimentally" determined single particle energies ε_j. The energy of the core E_o is taken to be constant and the core is assumed to remain inert. Thus the expectation energy of a Slater determinant is given by

$$\langle\psi|H|\psi\rangle = E_o + \sum_{j=A-n+1}^{A} \varepsilon_j + \sum_{i<j=1}^{A} \langle\phi_\alpha(r_i)\phi_\beta(r_j)|v_{ij}|\phi_\alpha(r_i)\phi_\beta(r_j) - \phi_\beta(r_i)\phi_\alpha(r_j)\rangle .$$

In our calculation, the interaction between all pairs of particles including those inside the core is taken into account and

$$\langle\psi_{\{\alpha\beta\}}|H|\psi_{\{\alpha\beta\}}\rangle = \sum_{i=1}^{A} T_i + \sum_{i<j=1}^{A} \langle\phi_{\alpha_i}(r_i)\phi_{\beta_j}(r_j)|v_{ij}|\phi_{\alpha_i}(r_i)\phi_{\beta_j}(r_j) - \phi_{\beta_j}(r_i)\phi_{\alpha_i}(r_j)\rangle.$$

There is no assumption of any single particle energies or the intrinsic energy of the core.

Since all particles are taken into consideration, the

total energy is a function of each of the α_i's, the oscillator constants of the different orbitals,

$$E = E(\alpha_1, \ldots, \alpha_A) \ . \qquad (2.9)$$

The α's, which are a measure of the nuclear size, are conventionally taken to have the same fixed value. However, we are involved in a variational calculation and the proper consistent values for the α's are those which give the lowest value for (2.9), subject to the constraint that the single particle states are orthonormal.

The Hamiltonian of the hypernucleus has the form

$$H = \sum_{i=1}^{A} T_i - T_{CM} + T_\Lambda + \sum_{i<j=1}^{A} v_{ij} + \sum_{i=1}^{A} v_{i\Lambda} \qquad (2.10)$$

where $v_{i\Lambda}$ is the lambda-nucleon interaction. The same procedure as that for the nucleus is employed. However, the Λ particle, with mass = 1115.57 MeV and T = 0, does not have the Pauli principle imposed on it, and it is not necessary to construct a wave function antisymmetric with the nucleons. The wave function for the A+1 particle system is therefore

$${}^{A+1}_{\Lambda}\Psi = \phi_\Lambda(r_\Lambda) \sum_P (-1)^P P \prod_{i=1}^{A} \phi_{\alpha_i}(r_i) . \qquad (2.11)$$

The Λ particle is assumed to be in a 1s state which can have generally different spatial extent than the 1s nucleon, i.e. α_Λ is generally different from α_1. Mathematically, this

is equivalent to the mixing of higher configurations to ϕ_Λ if $\alpha_\Lambda = \alpha_1$, i.e.

$$\phi_\Lambda(\alpha_\Lambda) = \sum_n C_n \phi_{\Lambda n}(\alpha_1).$$

α_Λ as well as the α_i is allowed to vary until the minimum value of the energy is reached.

In the minimization process, it is found that a better ground state can be achieved by allowing the system to deform. In order to investigate the effect of deformation, a representation of states such as the cylindrical harmonic oscillator single particle states $\psi_{n,m,n_z}(\rho,\phi,z)$ is used. $\psi_{n,m,n_z}(\rho,\phi,z)$ satisfies the equation

$$[-\frac{\hbar^2}{2M}\nabla^2 + \frac{M\omega^2}{2}\rho^2 + \frac{M\omega_z^2}{2}z^2]\psi_{n,m,n_z}(\rho,\phi,z) = E_{n,m,n_z}\psi_{n,m,n_z}(\rho,\phi,z) \tag{2.12}$$

where $$\rho^2 = x^2 + y^2,$$

and $$\psi_{n,m,n_z} = R_{n,|m|}(\sqrt{\alpha}\,\rho)\Phi_m(\phi)Z_{n_z}(\sqrt{\beta}\,z)$$

with
$$R_{n,|m|} = \left(\frac{2n!\alpha}{(n+|m|)!}\right)^{\frac{1}{2}}(\sqrt{\alpha}\rho)^{|m|}L_n^{|m|}(\alpha\rho^2)e^{-\alpha\rho^2/2} \tag{2.13}$$

$$\Phi_m = \frac{1}{\sqrt{2\pi}}e^{im\phi}$$

$$Z_{n_z} = \left(\frac{\beta^{\frac{1}{2}}}{\pi^{\frac{1}{2}}2^n z!}\right)^{\frac{1}{2}} H_{n_z}(\sqrt{\beta}\,z)e^{-\beta z^2/2}.$$

The energy $E_{n,m,n_z}(\alpha,\beta) = [(2n+|m|+1)\alpha+(n_z+\frac{1}{2})\beta]\hbar^2/M$. (Appendix 1)

The oscillator constants $\alpha \equiv M\omega/\hbar$, $\beta \equiv M\omega_z/\hbar$ determine both the size and the shape of the system. If $\alpha=\beta$, the deformed and the spherical representations are essentially identical (connected by an unitary transformation).

It is found that if the force gives saturation, the volume V remains almost constant during deformation. If we assume that the volume remains constant, then

$$V \sim 1/\alpha\sqrt{\beta} \ ,$$

i.e. $\alpha\sqrt{\beta} = c/V$, where c is the proportionality constant. Define $A \equiv (V/c)^{2/3}\alpha$, $B \equiv (V/c)^{2/3}\beta$, which are dimensionless, and $A\sqrt{B} = 1$. A deformation paramater d is defined as $d \equiv \sqrt{A/B}$. The state is prolate, spherical, oblate as

$$d \gtreqless 1.$$

Dependence of the energy on the deformation will now be considered. The total kinetic energy T_{n,m,n_z} is related to the total energy by E_{n,m,n_z} by

$$T_{n,m,n_z} = \frac{1}{2}E_{n,m,n_z} = \frac{1}{2}[(2n+|m|+1)\alpha+(n_z+\tfrac{1}{2})\beta]\hbar^2/M$$

$$= \frac{1}{2}\left(\frac{V}{c}\right)^{2/3}\frac{\hbar^2}{M}\left[(2n+|m|+1)A + (n_z+\tfrac{1}{2})\frac{1}{A^2}\right]. \qquad (2.14)$$

Minimization of T_{n,m,n_z} with respect to the variable A yields

$$\frac{dT_{n,m,n_z}}{dA} = (2n+|m|+1) - 2(n_z+\tfrac{1}{2})/A^3 = 0$$

which gives

$$A_{min} = [(2n_z+1)/(2n+|m|+1)]^{1/3} \qquad (2.15)$$

and the corresponding deformation

$$d_{min} = [(2n_z+1)/(2n+|m|+1)]^{1/2} \qquad (2.16)$$

(2.16) shows that $d_{min} \neq 1$ unless $n = m = n_z = 0$, i.e. the state [0,0,0] or $2n_z = 2n+|m|$. For other states, it can be concluded that the kinetic energy favours deformation, and the orbits will either prolate or oblate depending on the value of d_{min} . (Appendix 1).

A direct matrix element of the two-body potential $V(r_{12}/\gamma)$ can be expressed as

$$\int \psi^*_\mu(\sqrt{\alpha}\rho_1,\phi_1,\sqrt{\beta}z_1)\psi^*_\nu(\sqrt{\alpha}\rho_2,\phi_2,\sqrt{\beta}z_2)V(r_{12}/\gamma)\psi_\mu(\sqrt{\alpha}\rho_1,\phi_1\sqrt{\beta}z_1)$$

$$\psi_\nu(\sqrt{\alpha}\rho_2,\phi_2,\sqrt{\beta}z_2)\rho_1 d\rho_1 d\phi_1 dz_1\ \rho_2 d\rho_2\ d\phi_2\ dz_2 \qquad (2.17)$$

where γ is the range of the force. We note that α and β only appear in the wave functions in the form $\sqrt{\alpha}\rho$, $\sqrt{\beta}z$ except for the normalization constant where α and β occur in the combination $\alpha^{1/2}\ \beta^{1/4}$ which is proportional to $\frac{1}{\sqrt{V}}$, hence the normalization constant remains constant during the deformation.

The volume element can be written as

$\frac{1}{\alpha\sqrt{\beta}}[\sqrt{\alpha}\rho\ d(\sqrt{\alpha}\rho)d\phi\ d(\sqrt{\beta}z)]$, and if we define

$$x = \sqrt{\alpha}\rho, \text{ and } y = \sqrt{\beta}z$$
$$\gamma_\rho = \sqrt{\alpha}\gamma, \text{ and } \gamma_z = \sqrt{\beta}\gamma, \tag{2.18}$$

(2.17) can be written as

$$(\frac{1}{\alpha^2\beta}) \int \psi_\mu^2(x_1,\phi_1,y_1)\ \psi_\nu^2(x_2,\phi_2,y_2)V(x_{12}/\gamma_p, y_{12}/\gamma_z)x_1dx_1d\phi_1dy_1$$
$$x_2dx_2d\phi_2dy_2\ . \tag{2.19}$$

Since the integrations are over x,ϕ,y spaces, and $\alpha^2\beta$ is a constant, the only effective dependence of the matrix element on α and β is in the range parameters γ_ρ and γ_z which have different values. (2.19) is therefore equivalent to maintaining a spherical basis and employing a non-spherical potential. For the case of a spherical representation, i.e. $\alpha=\beta$, $\gamma_\rho=\gamma_z=\gamma_s$. For a prolate deformation, $\alpha>\beta$ and $\gamma_\rho>\gamma_s>\gamma_z$; namely the radial force has a range larger than the spherical range while the axial force range is smaller.

The matrix element (2.17) can be viewed as proportional to the overlap integral of two density functions and a variable range potential:

$$\int \rho_\nu(x_1,y_1)V(x_{12}/\gamma_\rho, y_{12}/\gamma_z)\ \rho_\mu(x_2,y_2)d^3\tau_1\ d^3\tau_2 \tag{2.20}$$

The behaviour of (2.20) when deformation occurs depends on the nature of the density distribution functions

ρ_μ and ρ_ν. If both the two particles are in spherical state e.g. [0,0,0] then whatever overlap is gained by increasing γ_ρ is compensated by the loss due to the decrease of γ_z and vice versa. Consequently (2.20) is insensitive to the deformation of the system.

If one of ρ is spherical, e.g. ψ = [0,0,0], while the other has $\bar{z}^2 > \bar{\rho}^2$ (Appendix 1), e.g. the state [0,0,1], then the increase of the overlap for increasing γ_z is more than the loss due to the decrease of γ_ρ; and (2.20) increases in magnitude. However, an increase in γ_z implies β has been increased, i.e. an oblate deformation occurs. Because the kinetic energy of such state favours a prolate deformation, an increase of β would result in increasing the kinetic energy. Thus potential binding is increased at the cost of increased kinetic energy which will overcome the gain in the total binding energy. An increase of γ_ρ decreases the potential energy of state like [0,0,1], but, a corresponding decrease in the kinetic energy just compensates the loss in potential energy. Similar argument holds for state having $\bar{\rho}^2 > \bar{z}^2$. Thus it can be said that the direct matrix elements of this type oppose deformation favoured by kinetic energy consideration.

If the two orbitals in (2.20) have different characters, i.e. one has $\bar{z}^2 > \bar{\rho}^2$ and the other has $\bar{\rho}^2 > \bar{z}^2$, there will be a cancellation of effects and the change due to deformation is small.

The exchange matrix element can be written as

$$\langle\psi_\mu(1)\psi_\nu(2)|V(\underset{\sim}{r}_{12}/\gamma)|\psi_\nu(1)\psi_\mu(2)\rangle$$
$$= \langle\psi_\mu(1)\psi_\nu(2)\ V(\underset{\sim}{r}_{12}/\gamma)P^x_{12}|\psi_\mu(1)\psi_\nu(2)\rangle$$

where the Majorana exchange operator P^x_{12} is defined by

$$P^x_{12}\ f(\underset{\sim}{r}_1,\underset{\sim}{r}_2) = f(\underset{\sim}{r}_2,\underset{\sim}{r}_1). \qquad (2.21)$$

If we transform $\underset{\sim}{r}_1$, $\underset{\sim}{r}_2$ into the relative and centre-of-mass co-ordinates $\underset{\sim}{r}$, $\underset{\sim}{R}$ by

$$\underset{\sim}{r} = \underset{\sim}{r}_1 - \underset{\sim}{r}_2\ ,\quad \underset{\sim}{R} = \tfrac{1}{2}(\underset{\sim}{r}_1 + \underset{\sim}{r}_2),$$

then $$P^x_{12}\ f(\underset{\sim}{r}_1,\underset{\sim}{r}_2) = P^x_{12}\ f(\underset{\sim}{r},\underset{\sim}{R}) = f(-\underset{\sim}{r},\underset{\sim}{R}). \qquad (2.22)$$

Consider a function $f(\underset{\sim}{r}+\underset{\sim}{r}_o,\underset{\sim}{R})$.

Letting $\underset{\sim}{r}_o = -2\underset{\sim}{r}$ gives $f(\underset{\sim}{r}+\underset{\sim}{r}_o,R) = f(-\underset{\sim}{r},\underset{\sim}{R})$ (2.23)

which, according to (2.22) is $P^x_{12}(r,R)$.

However $f(\underset{\sim}{r}+\underset{\sim}{r}_o,R)$ can always be expressed as a series having the form

$$f(\underset{\sim}{r}+\underset{\sim}{r}_o,R) = f(\underset{\sim}{r},\underset{\sim}{R}) + \underset{\sim}{r}_o\cdot\nabla_r\ f(\underset{\sim}{r},\underset{\sim}{R}) + (r_o\cdot\nabla_r)^2 f(\underset{\sim}{r},\underset{\sim}{R})/2!+\ldots$$

$$= e^{\underset{\sim}{r}_o\cdot\nabla_r}\ f(\underset{\sim}{r},R)\ . \qquad (2.24)$$

(2.23) and (2.24) together give

$$P^x_{12} = e^{-2\underset{\sim}{r}\cdot\nabla_r} = e^{\,i2\underset{\sim}{r}\cdot\underset{\sim}{P}/\hbar} \qquad (2.25)$$

where $\underset{\sim}{P}$ is essentially the relative momentum operator except that it commutes with $\underset{\sim}{r}$ in the exponential.

The exchange matrix element can be taken as a direct matrix element with the interaction multiplied by an oscillatory factor $e^{2i\underset{\sim}{r}_{12}\cdot\underset{\sim}{P}_{12}/\hbar}$. An oscillatory factor will in general reduce the magnitude of the integral in which it occurs, and this explains why the exchange matrix element is always less than the direct matrix element. The larger the relative momentum, the greater the cancellation effect of the oscillating term will be.

As for effect of deformation, consider again the orbital [0,0,1], a decrease in β will result in making it more prolate, thus decreasing the kinetic energy. The relative moment and hence the oscillating factor is therefore reduced leaving a larger exchange matrix element. It is found from explicit calculation that the effect of the oscillatory factor is more important than the range effect discussed with respect to the direct matrix element. Consequently, the exchange matrix element favours deformation as does the kinetic energy.

The variation of the 1s,1p matrix elements as a function of deformation is given by Volkov[9]. Examination of these matrix elements shows that from the energy point of view, many systems prefer a deformed representation.

For a non-spherical system, the total angular momentum J is no longer a good quantum number. However, for comparison purposes, it is desirable to use a basis in the deformation calculation which will give the conventional intermediate coupling results in the limit of zero deformation. This can be done by using a Slater determinant representation characterized by the total M value (z-component of angular momentum) of the system. As long as the system has cylindrical symmetry, the Hamiltonian does not connect states of different M, and it can be diagonalized separately for each M basis. In the zero deformation limit the results are identical to those obtained from a spherical representation, and the appropriate J for any given level can generally be determined by a simple counting of the number of degenerate states for the particular level.

CHAPTER 3

THE LAMBDA-NUCLEON AND THE NUCLEON-NUCLEON POTENTIAL

Since the introduction by Yukawa of the meson-exchange process, it has been accepted that the strong interaction between baryons is generated by the exchange of one or more mesons. Unlike the nucleon-nucleon case the Λ-N interaction involves a two-channel process (Fig. 1a). Thus, the simplest single-channel Λ-N potential includes at least two-pion exchange (TPE) as shown in Fig. 1b. The effect of two-pion exchange processes is similar to the effect of the exchange of a single scalar T=0 particle which gives rise to a static attractive central potential with a very strong spin-independent part. The spin-dependent terms are typically two orders of magnitude smaller.

K-meson exchange (OKE) (Fig. 1d) also contributes directly to the Λ-N potential. The exchange of a T=1/2 particle leads to an exchange potential which contains the factor $(-P^{x}P^{\sigma})$, where P^{x} and P^{σ} are the space and spin exchange operators respectively. P^{σ} operating on a singlet state changes its sign but keeps the triplet wave function unaltered, i.e.

$$P^{\sigma}|\text{singlet}\rangle = -|\text{singlet}\rangle$$
$$P^{\sigma}|\text{triplet}\rangle = |\text{triplet}\rangle ,$$

while P^{x} reverses the sign of relative coordinate of states of odd L[13]. The OKE contribution can produce a p-state suppression in the Λ-N force. OKE also generates a strong tensor potential though as yet no experimental verification of this tensor potential is available.

Multi-meson exchanges should be included as well, but owing to the short range and the complication of such contributions theoretical progress on this question is small.

Instead of treating the multi-meson exchange mechanism in detail, an alternate approach, the one-boson-exchange (OBE) model, has been proposed. The underlying argument is that multi-meson exchange processes are dominated by resonances, and that such a resonance can be treated approximately as a single particle. A complete description of this model was given by Downs and Phillips[13]. Using this approximation and SU_3 symmetry, Deloff[14] was able to reproduce the scattering data, though not the correct hypernuclear binding.

Since the dominant attractive contribution to the potential comes from two-pion exchange or its equivalent, the intrinsic range b of the Λ-N interaction might be expected to be about 1.5 fm. However, the calculations of Downs and Phillips suggest that a more appropriate value of b would be larger than this. Ali et

al.[15] have also noted that the equality of the single and triplet scattering parameters requires a longer intrinsic range. They found that the best fit to the scattering data (1966) required b to be 2.07 fm, whereas the corresponding value suggested by Alexander and Karshon[16] for the 1967 data is about 1.8 fm. An acceptable explanation for the large intrinsic range is the existence of a hard core, since the overall intrinsic range b is related to the intrinsic range b_o of the attractive part by

$$b_0 \simeq b - 2r_c$$

where r_c is the hard-core radius. The presence of a hard core with $r_c \gtrsim 0.3$ fm in the Λ-N potential as well as the tendency towards a large intrinsic range (b>1.5 fm) have also been verified by Herndon and Tang[17]. The absence of a bound hyper-deuteron leads to an upper limit of core radius of about 0.6 fm.

An interaction with an infinite core can not be used in a shell model calculation since the matrix elements are infinite in such cases. A similar situation occurs in the nucleon-nucleon interaction; and, to overcome this difficulty, the G matrix has been introduced[18]. The matrix G is defined to be

$$\langle k_1,k_2|G|i_1,i_2\rangle=\langle k_1k_2|v_{ij}|i_1i_2\rangle-\sum_{m_1m_2>k_F}\frac{\langle k_1k_2|v_{ij}|m_1m_2\rangle}{e}\langle m_1m_2|G|i_1i_2\rangle \qquad (3.1)$$

where v_{ij} is the two-body potential, k_F the Fermi momentum, and e the energy denominator defined as

$$e = e_{m_1} + e_{m_2} - e_{i_1} - e_{i_2}$$

e_{m_1}, e_{m_2}, e_{i_1}, e_{i_2}, are the single particle energies of particles having momenta m_1, m_2, i_1, i_2.

An exact solution of (3.1) is possible in principle, but it is very difficult in practice. Approximation methods have been developed, such as the Moszkowski and Scott (MS) separation method[20]. The interaction v_{ij} is split into a short and a long range part characterized by a separation distance d. The long-range part v_ℓ of the potential is well-behaved, while the short-range part, v_s, gives a repulsive contribution G_s which is called the dispersion term by MS. Details of the derivation are omitted here but it can be proved that

$$G_s = G_s^{(0)} \frac{Q-1}{e} G_s^{(0)} + G_s^{(0)} \left(\frac{1}{e} - \frac{1}{e^o}\right) G_s^{(0)} \qquad (3.2)$$

where Q is the Pauli projection operator, e^o is the same energy denominator as for free particles of the same momenta. $G_s^{(0)}$ defined by $G_s^{(0)} = v_s - v_s \frac{1}{e} G_s^{(0)}$ is an approximation to G_s.

The long range part of the potential is approximated by a Volkov type force; i.e., the Λ-N potential is taken to be the sum of an attractive and a repulsive Gaussian (Fig. 2).

This choice of shape is taken for mathematical simplicity rather than for any physical reason. Dalitz and Downs have shown that, for low energy interactions, the shape dependence is negligible. This result will also be verified in this work. The potential is of the form

$$v_{N\Lambda} = (V_a\, e^{-r^2/r_A^2} + V_r\, e^{-r^2/r_R^2})(w_\Lambda + m_\Lambda\, P^x) \qquad (3.3)$$

$$w_\Lambda + m_\Lambda = 1$$

where V_a, V_r are the strengths, w_Λ and m_Λ are the Wigner and Majorana exchange parameters, values of which are adjusted to give the required p-state suppression.

The separation distance d is momentum-dependent. r_R in (3.3) is, in a way, a measure of this separation; and, consequently it can be made a function of the relative momentum k of the two interacting particles. The functional form of r_R with respect to k is rather arbitrary. Here it is assumed to be

$$r_R = r_{RO}\,(1 + C_\Lambda k^2), \qquad (3.4)$$

where C_Λ is used as a parameter which has to be determined in some manner.

V_a, V_r, r_A, r_R are chosen to fit the free particle Λ-N parameters at low energies, $(V_a + V_r)$ is kept to some small value in order to make the radial shape similar to a Moszkowski and Scott type v_ℓ potential; r_A as mentioned above corresponds to an intrinsic range of 1.7 to 2.1 fm approxi-

mately. Satisfying these requirements reduces the arbitrary nature of the potential (2.3).

The scattering lengths a_s, a_t and the effective ranges r_s, r_t for the singlet and triplet state were obtained from the $\sigma_{\Lambda p}$ scattering cross-section by use of the four-parameter equation

$$\sigma_{\Lambda p}=\frac{1}{4}\sigma_s+\frac{3}{4}\sigma_t = \pi/[k^2+(-\frac{1}{a_s}+\frac{1}{2}r_s k^2)^2]+3\pi/[k^2+(-\frac{1}{a_t}+\frac{1}{2}r_t k^2)^2]$$

where k is the relative wave number. This relation is valid for incident Λ laboratory momenta in the region $120<P_\Lambda<320$ MeV/c. The Maryland and Rehavoth-Heidelberg groups both performed experiments on low energy Λ-p elastic scattering, and their results agree with each other quite well. For higher energies r_R is k-dependent and C_Λ in (2.4) is fixed so as to give the correct $\sigma_{\Lambda p}$ (Fig. 3). However, the scarcity and uncertainty of the high energy (>30 MeV) data prevents an accurate determination of C_Λ. Fortunately C_Λ is so small that reasonable variation of its value has no important effect on the binding and spectroscopic calculations.

A Majorana space exchange term is necessary in order to account for the K meson exchange. Herndon and Tang[17] have shown in their s-shell hypernuclear binding and Λp scattering calculations that the potential strength in odd-parity states should be 60% of that in even states . Since $w_\Lambda+m_\Lambda=1$, a 40% suppression of the odd L state requires

the $m_\Lambda = 0.2$, whereas a Serber type force has $m_\Lambda = 0.5$. Since there is no theoretical justification for the values of m_Λ, it is treated as a parameter and the dependence of the Λ-binding energy on m_Λ shall be studied.

The expected density-dependence in the Λ-N interaction should arise primarily from the short range repulsive interaction mentioned previously and from the short range tensor force which in the case of the nuclear tensor interaction can be approximated by a density dependent effective central potential as shown by Kuo and Brown[21]. The density dependence can also approximate the effect of ΛNN forces expected from meson theory.

G_s in (3.2) consists of the Pauli and the spectral correction terms $G_s^{(0)} \frac{Q-1}{e} G_s^{(0)}$ and $G_s^{(0)} \left(\frac{1}{e} - \frac{1}{e_o}\right) G_s^{(0)}$ respectively. Since the interaction is very strong at short range, the particle will most probably be scattered out of the Fermi sea. The Pauli correction is therefore negligible, leaving only the spectral correction. Therefore, G_s is nearly proportional to the difference $e - e_0$. But

$$e-e_0 = e_{m_1} + e_{m_2} - e_{i_1} - e_{i_2} - (k_{m_1}^2 + k_{m_2}^2 - k_{i_1}^2 - k_i^2)$$

$$= U(m_1) + U(m_2) - U(i_1) - U(i_2)$$

where $U(m_1)$, $U(m_2)$, $U(i_1)$, $U(i_2)$ are potential energies of the particles in the states m_1, m_2, i_1, i_2 respectively. As m_1, $m_2 > k_F$, the particles are at the top of the potential well and $U(m_1)$, $U(m_2)$ are small. As far as i_1 and i_2 are concerned, one of them say i_1 represents the Λ particle, which having no Pauli principle imposed on it, always remains at the bottom of the well and has a potential energy equal to the well depth D_Λ;while $U(i_2)$, the hole potential energy, is of the order of the average potential of a nucleon. The average potential energy of occupied states is given by the well known relation

$$\bar{U}_{\ell sJ} = 12\rho \int_0^1 x^2(x-1)^2(x+2)\bar{G}_{\ell sJ}(xk_F)dx \qquad (3.5)$$

where $\bar{G}_{\ell sJ}$ is the averaged diagonal element which is related to the G matrix by

$$\bar{G}_{\ell sJ}(k) = 4\pi \frac{\hbar^2}{M} \frac{(2J+1)(2T+1)}{8} G^J_{\ell,\ell}(k,k) \text{ MeV fm}^3,$$

and k_F is proportional to $\rho^{1/3}$. Integrating (3.5) over x shows that the average potential energy is function of the density ρ. Thus it can be concluded that the relation

$$G_S \sim \rho^n$$

which Bethe[19] suggested for N-N case is also applicable to the Λ-N force.

Nuclear matter calculations suggest that $n \sim 1$ is

probably a reasonable choice. For hypernuclei involving light nuclei cores, nuclear matter predictions have to be modified. It is probably appropriate to take n as a parameter to be determined by the appropriate criteria.

The other source of the density dependence arises from the tensor force. Law, Gunye and Bhaduri[22/] approximate the Λ-N tensor force by an effective central term of the form

$$W_{eff}(r,k_F) = -\left(\frac{M}{\hbar^2}\right)\frac{3}{2\pi}W_T(r)S_{1\Lambda}^2(r)\int_0^\infty Q(r,r')W_T(r')r^2dr'$$

where

$$Q(r,r') = \frac{k_F^2}{\Delta}\int_0^\infty F(s,\delta,U_1')j_2(k_Frs)j_2(k_Fr's)sds \text{ and}$$

s,δ,U_1' are functions of k_F.

The potential W_{eff} is difficult to deal with unless some assumptions are made. However, the main purpose of presenting W_{eff} here is to indicate that the tensor force can be approximated by a k_F-dependent effective term. The Fermi momentum k_F is in turn related to the nuclear density by

$$\rho = \left(\frac{2}{3\pi^2}\right)k_F^2$$

therefore $W_{eff} = W_{eff}(r,\rho)$.

Since both the G_s and the tensor force have a range shorter than the two-pion exchange range, phenomenologically their effect can be summed up in making V_r, the depth of the short term, density dependent. A form

$$V_r = [1 + C_{\Lambda 4}\, \rho^n\, (\underset{\sim}{r}_N)]V_{ro}(\underset{\sim}{r}_N - \underset{\sim}{r}_\Lambda) \qquad (3.6)$$

is used, where $C_{\Lambda 4}$ and n are taken as parameters determined by fitting D_Λ, the binding energy of the Λ particle in nuclear matter.

The Λ binding in nuclear matter is calculated by first order perturbation, with a force fitting the two-body scattering. If $m_\Lambda = C_\Lambda = C_{\Lambda 4} = 0$, then D_Λ is found to be 86 MeV, rather close to the 90 MeV given by Bhaduri, Nogami and Van Dijk[23/]. D_Λ is sensitive to the value of m_Λ (Fig. 4). This is understandable, since the odd state suppression does reduce the Λ-binding considerably.

The generally accepted 'experimental' value of D_Λ is about 30 MeV. Much work[24/] has been done to obtain this value. However, the accuracy of D_Λ is subject to question. Recently Bhaduri et al[25/] have pointed out that if a three-body force is included, the argument which leads to D_Λ = 30 MeV is no longer valid. Their reason is that the expression used to deduce D_Λ from the measured B_Λ, $B_\Lambda = D_\Lambda - \frac{\pi^2 \hbar^2}{2m_\Lambda r_o^2} A^{-2/3}$ is only true for a two-body interaction.

Bhaduri and Law[26/] have deduced D_Λ directly from scattering data, and they have found that D_Λ should be 60 MeV which doubles the previous value. If it be the case, then the value of m_Λ would be less than 0.25 as seen from Fig. 4.

The density term helps to decrease D_Λ, and Fig. 4 gives the relation between D_Λ and $C_{\Lambda 4}$ for different m_Λ. It is seen that D_Λ decreases more or less linearly with an increase of $C_{\Lambda 4}$. However, $C_{\Lambda 4}$ has to be rather large to reduce D_Λ to 30 MeV.

The nuclear density is approximated by $\rho = \rho_o \exp(-\alpha r^2)$, where r is the coordinate of the nucleon. Only the nuclear density appears in the ΛN density dependent potential term since this is implicit in the theoretical arguments given above.

Spin dependence of the Λ-N interaction has long been a subject of investigation. The s-shell hypernuclear binding indicates a fairly strong spin-dependence because of the ratio $|a_s/a_t| \sim 4$. The analysis of these light hypernuclei is as follows.

The experimental value of the volume integrals U_2 and U_4 are derived from the Λ binding energies of ${}^{3}_{\Lambda}H$ and ${}^{5}_{\Lambda}He$. U_2 and U_4 are found to be 660±45 and 925±45 MeV fm^3 respectively. The volume integrals U_s and U_t of the singlet and triplet potential are related to U_2 and U_4 by

$$U_2 = \frac{3}{2} U_s + \frac{1}{2} U_t,$$

$$\text{if } U_s > U_t.$$

$$U_4 = U_s + 3U_t ,$$

This gives U_s = 380 MeV fm^3 and U_t = 180 MeV fm^3. The

singlet is much stronger than the triplet interaction. However the scattering lengths are very close to each other for the singlet and triplet interaction. The potential obtained from scattering yields a U_s only slightly stronger than U_t, contradicting the result obtained from the binding energy derivation.

The density dependence discussed in this chapter is able to remove part of the discrepancy without explicitly introducing spin dependence into the potential obtained from scattering. U_s and U_t are calculated with (A2.11) which gives U_s = 414.57 MeV fm^3, U_t = 402.42 MeV fm^3 for $C_{\Lambda 4}$ = 0.0. When the density term $C_{\Lambda 4}\rho^3$ is added, it is found that U_s = 397.07 MeV fm^3 and U_t = 364.24 MeV fm^3, for $C_{\Lambda 4}$ = 136.0. The ratio U_s/U_t goes from 103% to 109% which indicates that the density dependent term has made the potential more spin dependent. However, it should be pointed out that the choice of the same density dependence for both the singlet and triplet potentials is completely arbitrary.

The existence of isomeric states of $^{7}_{\Lambda}$He provides another check of the spin dependence. Dalitz and Gal[27] have shown that if the difference in the potential matrix element, (V_s-V_t), is greater than 0.25 MeV, then neither the 7/2+ nor 5/2+ state would be isomeric. Thus existence of the isomeric state furnishes an upper limit to the difference between the singlet and triplet potential energy.

Though the scattering parameters for the singlet and triplet interaction only differ slightly, the singlet and triplet potentials are given explicitly in this work. The ΛN force used throughout this thesis is of the form

$$v(r,\rho)=[V_a\, e^{-r^2/r_A^2} + V_{ro}(1+C_{\Lambda 4}\rho^n)e^{-r^2/r_{Ro}^2(1+C_\Lambda k^2)^2}][w_\Lambda+m_\Lambda P^x]$$

with

	V_a	V_r	r_A	r_{RO}	$w_\Lambda + m_\Lambda$
singlet	-55	60	1.2	0.7	1
triplet	-68	73	1.2	0.85	1

For hypernuclear binding calculations, the choice of a nucleon-nucleon potential is important since the Λ-binding energy is sensitive to the nuclear size, and the excited states of the hypernuclei are closely related to those of the nuclear core.

It is well-known that low-energy nuclear properties are rather independent of the shape of the potential. It is not necessary for the N-N force to have the same shape as the Λ-N force, but it is convenient, when calculating the Λ-N and N-N matrix elements, to use a gaussian form for both potentials.

The Tabakin potential has been employed by Bassichis and Gal[40] for calculation of the p-shell hypernuclear binding energies. However, as pointed out by the authors, the assumption of the

calculation is that the variation of the Λ wave function with the nuclear mass number A should be negligible, whereas in the actual calculation the Λ wave function changes due to the poor saturation properties of the Tabakin potential. Law, Gunye and Bhaduri[22/] in their $^{5}_{\Lambda}$He Hartree-Fock calculation used both the Yale and Volkov potential. The former potential is found to give too large a rms radius and too small a binding energy for the α-particle unless the triplet reduced matrix element is increased by 30%. The latter potential, though leading to a correct size and binding energy,does not saturate nuclear matter.

A criterion in choosing a N-N potential for the hypernuclear core is the fitting of the rms radius and the binding energy of the nucleus. Furthermore, a N-N force has to satisfy strictly nuclear criteria such as saturating nuclear matter at the correct density, giving the correct energy per particle and the singlet and triplet scattering phase shifts, etc. It is found that it is difficult to determine an effective potential which satisfies all these conditions and which also gives the required size and binding for nuclei from ^{4}He to ^{12}C. A force can always be artificially constructed to produce the right size while discarding some of the other required properties. However, one purpose of hypernuclear studies is to have a better understanding of the dynamical

relation of the nuclear core to the Λ particle binding, and too artificial a N-N potential cannot lead to any meaningful conclusion about the nucleus. Hence a 'realistic" effective N-N potential is insisted upon throughout the whole investigation.

The N-N potential employed is a modification of the two-Gaussian Volkov type of potential which is made density dependent by multiplying both the long range attractive and short range repulsive terms by appropriate factors. The force used is then of the form

$$v_{ij}=[-250(1+C_3\rho^{1/3})e^{-r^2/1.5^2}+255(1+C_4\rho^3)e^{-r^2/\lambda_R^2}][w+mP^x+bP^\sigma+hP^\tau]$$

where $\lambda_R = 1.247\ [1 + 0.15\ (k-0.836)^2]$,

and $w = 0.5,\ m = 0.5,\ b = 0.075,\ h = -0.325.$

In the zero density limit this is an appropriate phase fitting force, while the density factors insure the saturation properties of nuclear matter.

The origin of the density dependence has been discussed earlier for the Λ-N force. Phenomenologically in addition to the density term $C_4\rho^3$ a term $C_3\rho^{1/3}$ is added to the long range part which might be attractive or repulsive depending on C_3 is positive or negative.

The local density approximation with a small correction has been found to be valid for large systems[19]. It is assumed that the density ρ is a function of the centre-of-mass

coordinate R alone; i.e. $\rho=\rho(\underset{\sim}{r}_1+\underset{\sim}{r}_2)$. If ρ is taken to be a gaussian distribution then $\rho=\rho_o\, e^{-\frac{1}{2}\alpha(\underset{\sim}{r}_1+\underset{\sim}{r}_2)^2}$ where $\underset{\sim}{r}_1$ and $\underset{\sim}{r}_2$ are the coordinates of the two nucleons. For light nuclei this approximation appears to over suppress the potential. For instance, ^{4}He is almost all surface and taking $\rho=\rho(\underset{\sim}{R})$ essentially always leads to an over estimate of the local density because of the central peaking of the density distribution. The local-particle approximation would seem to be more appropriate for these nuclei. In this case ρ is taken to be the geometrical mean of the co-ordinates of the individual particle, $\rho=\rho_o\, e^{\frac{1}{2}\alpha(r_1^2+r_2^2)} = \rho^{\frac{1}{2}}(r_1)\rho^{\frac{1}{2}}(r_2) = \rho(\sqrt{r_1^2+r_2^2})$ for the gaussian density distribution. For all but the lightest nuclei either approximation gives similar results.

The coefficients C_3, C_4 are adjusted to give the nuclear matter binding energy and density (B.E. = 16 MeV per particle, k_F = 1.36 fm^{-1}). Since the force is quite density dependent (the repulsive part has a term $\sim \rho^3$), the compressibility in nuclear matter is rather high $\sim$ 400 MeV. Calculated binding energies and rms radii are compared with the experimental values in Table 2. The experimental rms radii are taken from two sources. One is from a 1966 analysis of the data[29/] on scattering, proton binding energies and the Coulomb energy. An average is taken and the values $\langle r^2\rangle^{\frac{1}{2}}$ are obtained by correcting for the centre-of-mass. The other entries are from the Hofstadler data[30/] deduced from electron

TABLE 2

The binding energies and the root mean square (rms) radii of the p-shell nuclei

Nucleus	Binding Energies (in MeV)		rms radius (in fm)		
	Experimental	Calculated	Experimental (ref. 29)	Experimental (ref. 30)	Calculated $\langle r^2 \rangle^{\frac{1}{2}}$
^{5}He	27.34	25.49	2.32 ± 0.28	-	2.165
^{6}He	29.24	24.94	-	-	2.360
^{6}Li	31.99	32.03	2.38 ± 0.12	2.78	2.447
^{6}Be	-	32.04	-	-	2.447
^{7}Li	39.24	39.11	2.36 ± 0.16	2.71	2.53
^{7}Be	37.60	39.12	-	-	2.53
^{8}Be	56.50	58.15	2.17 ± 0.17	-	2.63
^{8}Li	41.28	35.74	-	-	2.63
^{10}B	64.75	62.62	2.26 ± 0.13	-	2.64
^{11}B	76.21	70.10	2.24 ± 0.11	-	2.66
^{12}C	92.16	89.70	2.32 ± 0.10	2.37	2.66

scattering (1965).

For light p-shell nuclei e.g. ^{6}Li, ^{7}Li, the rms radii are overestimated by the force. However, the calculated $\langle r^2 \rangle^{\frac{1}{2}}$ increases with A, whereas the observed values change only slightly as A increases. A comparison between the two sets of data indicates that considerable uncertainty still exists in the experimental rms radii and it is not too meaningful to try to fit either of the values too exactly.

CHAPTER 4

THE BINDING ENERGIES OF $^{5}_{\Lambda}$He AND ITS CORE

The study of both ^{4}He and $^{5}_{\Lambda}$He is of great interest. The α-particle is the lightest closed-shell nucleus and is closely packed with a rms ardius of about 1.7 fm. $^{5}_{\Lambda}$He is the hypernucleus with a ^{4}He core and the Λ binding energy 3.08 ± 0.03 MeV is by far the most accruately determined B_{Λ} value.

The four nucleons of ^{4}He spend most of their time as 1s particles. However, if particle-hole excitations are allowed, it is found that small configuration mixing occurs. This not only affects the binding energy of the α particle, but also affects the corresponding Λ binding energy. The calculated B_{Λ} can be increased by about 20%. Furthermore, a spectroscopic calculation of excited states can only be accomplished with core excitation. Hence it is important to extend the basis set wave functions to include higher shells (e.g. 2s1d).

The various effects of the core polarization are presented in Table 4. The potentials used for this calculation are force A and C in Table 3. Table 4 lists the probability that the α-particle is in the 1s, 1p, 2s1d shell. Although the wave function varies with the force

TABLE 3

The N-N force constants

$$\nu_{ij} = [V_A(1+C_3\rho^{1/3})\, e^{-r^2/\lambda_A^2} + V_R(1+C_4\rho^n)e^{-r^2/\lambda_R^2}][\omega+mP^x+bP^\sigma+hP^\tau]$$

$$\text{where } \lambda_R = \lambda_R^0\,[1 + C_1(k-C_2)^2]$$

	n	ν	C_3	C_4	b	h
A	2.0	-1.0	-0.1724	1.5122	0.1375	-0.2625
B	2.0	-1.5	-0.1392	1.5999	0.10625	-0.29375
C	2.0	-2.0	-0.1061	1.6437	0.075	-0.325
C'	2/3	-2.0	0.12731	0.76869	0.075	-0.325
C"	3.0	-2.0	-0.1292	6.002	0.075	-0.325
D	2.0	-3.0	-0.0324	1.6680	0.0125	-0.3875

$\nu = 10\ (\omega-m) + 8(b+h)$

$V_A = -250.0$, $V_R = 255.0$, $\lambda_A = 1.5$, $\lambda_R^0 = 1.247$

$C_1 = 0.15$, $C_2 = 0.836$, $m = 0.5$

used, the 1s character of the wave function is always more than 90%.The calculated binding energy increases by 0.8 ∿ 1.6 MeV with the correlated wave function. The rms radius for both uncorrelated and correlated wave function is given. When higher orbitals are included, a decrease in the rms radius is obtained. This is not too surprising since mixing of higher configurations is equivalent to building up a longer tail in the wave function. However, since the wave function is normalized,(i.e. the area under the distribution curve is constant),a longer tail results in decreasing the density of the inner and intermediate parts which reduces the cross-terms in the expression (A3.4). The diagonal matrix elements of the tail are too small to compensate for the reduction occurring in the cross-terms. Consequently, ^{4}He has a smaller calculated rms radius when the basis is extended.

It should be emphasized that when there is particle-hole excitation, the centre-of-mass energy has to be taken care of, otherwise spurious states would be introduced. Detailed treatment of the centre-of-mass energies is given in Appendix 4.

One of the criteria for selecting a N-N potential for light nuclei is the fitting of ^{4}He binding energy and size in a variational equilibrium calculation. The experimental α binding energy 28.296 MeV is well-established, but

TABLE 4

Properties of ^{4}He with the simple and correlated wave function

FORCE	Wave function	Probability of α-particle in %			Binding Energy (MeV)	rms radius (fm)
		1s	1p	2s1d		
A	simple	100	0	0	24.63	1.99
	Correlated	91.834	2.729	5.437	25.47	1.97
C	Simple	100	0	0	31.12	1.89
	Correlated	92.199	2.544	5.257	32.71	1.87

there is still some disagreement on the rms radius. Two recently reported values are 1.71[31/] and 1.68±0.05 fm[32/]. The former value is a fit to the charge form factor of ^{4}He, while the latter is from the measurement of π^- - ^{4}He and π^+ - ^{4}He elastic scattering

Theoretical calculations have been performed to reproduce the ^{4}He data. The Volkov force[9/] was formulated to give the correct ^{4}He size and binding, but it fails to reproduce both the nuclear matter data and the ^{4}He energy spectrum. Other investigators[33,34,35/] have studied the negative parity states, and though some success has been achieved, none of these authors has tried to calculate a self-consistent nuclear size.

In order to reproduce the experimental data, both the value of ν and n in the NN force were allowed to vary (see Table 3). However, the corresponding C_3, C_4 must then be adjusted so as to satisfy the restrictions imposed by nuclear matter.

The calculated binding energy B(^{4}He) increases as ν becomes more negative. Fig. 6 shows the variation of the calculated binding energy with respect to the rms radius $\langle r^2 \rangle^{\frac{1}{2}}$ as determined by using different values of ν. The relation is almost linear, and it appears that it is impossible to obtain a force giving both the correct size and binding energy simply by changing ν.

Increasing the density dependence also affects $B(^4He)$ and $\langle r^2 \rangle^{\frac{1}{2}}$. If n is treated as a parameter, then both $\langle r^2 \rangle^{\frac{1}{2}}$ and $B(^4He)$ decrease as n is increased. However, the decrease is relatively greater for the binding energy (Table 5); thus it is not possible to reduce $\langle r^2 \rangle^{\frac{1}{2}}$ to its correct value without underbinding ^4He. n is restricted, somewhat arbitrarily, to be less than or equal to three since the usually assumed value, obtained from nuclear matter calculations, is $n = \frac{2}{3}$. Since the average density of ^4He is less than the density of nuclear matter, it does not seem unreasonable to use n as a parameter to be determined by the properties of ^4He.

It should be noted in the second part of Table 5 that the properties of ^4He are relatively insensitive to changes of n as it is increased from $\frac{2}{3}$ to 3. This is due to the fact that C_3 and C_4 must be modified as n is changed in order to give the correct results for nuclear matter. The density dependence of the N-N force, as opposed to the exchange dependence v, is self compensating in the sense that the nuclear matter criteria are enough to virtually fix the qualitative results for finite nuclei.

The ^4He spectrum is given in Fig. 5. The 0^+ state at 28.1 MeV excitation energy is high compared to the experimental value[36]; however, it is still an improvement

TABLE 5

(a) Properties of ^{4}He with different exchange dependence

FORCE	ν	B(^{4}He)	0^+ excitation energy	rms radius
A	-1.0	25.47	24.51	1.97
B	-1.5	28.95	26.79	1.92
C	-2.0	32.71	20.16	1.87
D	-3.0	42.25	35.07	1.77

n = 2

(b) Properties of ^{4}He with different density dependence

FORCE	n	B(^{4}He)	0^+ excitation energy	rms radius
C'	2/3	35.72	29.80	1.92
C	2	32.71	29.16	1.87
C"	3	31.45	29.01	1.86

ν = -2.0

on the 40 MeV above the ground state obtained from simple phase fitting force. The 2^- and 1^- states agree pretty well with the observed levels. The 0^- state is rather high, an explanation for this is that ^{4}He, which is spherical in its ground state, may have deformed excited states; and a gain of a few MeV by deformation is very plausible.

Force C" ($\nu = -2$, $n = 3$) yields a binding energy* nearly equal to the correct value. Nevertheless, with this force the rms radius is still too large. If the experimental value is taken to be 1.71 fm, then the calculated one is 9% too large. For hypernuclear binding energies such an error in the rms value cannot be ignored, and a size correction is essential to obtain an absolute value of the binding energy. Attempts have been made to reduce the calculated size; and while a decrease in ν leads to an acceptable radius, it also gives too high a binding energy and a poor spectrum of excited states in which the 0^+ would be $\sim$ 35 MeV (Force D in Table 3).

A "realistic" force leading to the correct calculated size, binding energy and spectrum is hard to obtain. Force C" appears to be the best in this approach and it will be used for the nuclear core in the $^5_\Lambda$He calculation.

---

*The Coulomb interaction would reduce the calculated energy to about 29 MeV.

The theoretically predicted Λ binding energy in $^{5}_{\Lambda}$He has always been too large[15,17,23] compared with the experimental value. Several reasons have been suggested for the discrepancy. They are:

1) The existence of a tensor force in the triplet component of the Λ-N force, since $^{5}_{\Lambda}$He is a spherical system in which the tensor force should be suppressed;

2) Isospin suppression, which has two possible origins. Fig. 1 shows that, after exchanging a pion, the (Λ-^{4}He) system goes to the (Σ-^{4}He) channel. Σ has isospin equal to 1, so in order to have isospin conservation, ^{4}He should be in one of the T=1 excited states which are at least 22 MeV about the ground state. If this is treated by second order perturbation theory, second order energy

$$\sum_{j} \frac{\langle\psi_i|V|\psi_j\rangle\langle\psi_j|V|\psi_i\rangle}{e_j - e_i}$$

will have an energy denominator $e_j - e_i \geq m_\Sigma - m_\Lambda + 22$ MeV, where $m_\Sigma - m_\Lambda = 77$ MeV is the mass difference between the Σ and Λ. The energy denominator for $^{5}_{\Lambda}$He is increased by 28.6% compared to the smallest free interaction energy denominator. Thus, all free energy terms from 77 MeV $\leq e_j - e_i \leq$ 99 MeV are excluded for the $^{5}_{\Lambda}$He case and a resultant decrease in the second order contributions could be expected.

3) Charge symmetry breaking with which the binding energies of $^{4}_{\Lambda}$He and $^{4}_{\Lambda}$H indicate the Λn force is weaker than the Λp force;

4) The presence of a ΛNN three-body force which has been theoretically calculated to be repulsive, and which is therefore especially important for overbound hypernuclei;
5) The effect of the short range interaction as described in Chapter 3 of this thesis.

Bhaduri, Loiseau and Nogami[51] have considered the three-body force aspect of the problem with some success, but the uncertainty in the ΛNN interaction leads to only qualitative results at best. Law, Gunye and Bhaduri[22] have performed Hartree-Fock calculations with the tensor force and have concluded that the tensor force effect is not sufficient to reduce the Λ binding energy to the correct value. Herndon and Tang[17] have taken the charge symmetry breaking effect into account, but overbinding persists.

As a starting point in these calculations, a central two-body potential is employed and the Λ binding energy is determined in several ways:

1) A simple variational calculation in which an antisymmetrical wave function, a Slater determinant with all the nucleons and the Λ particle in 1s states is minimized with respect to the ground state energy by finding the optimum oscillator constants. The difference

in the ground state energy between the hypernucleus and the core gives the Λ binding energy;

2) A variational and configuration mixing minimization of the binding energy as described in Chapter 2 is performed, in which core excitations (1 particle-1 hole to the 2s1d and 2 particle-2 hole to the 1p shell) are allowed;

3) The rigid α model in which the average Λ potential $V_\Lambda(r_\Lambda)$ is the overlap integral of the nucleon single particle density with the Λ-N potential; and the Λ binding is obtained by solving exactly the Schroedinger equation with $V_\Lambda(r_\Lambda)$. (Appendix 2).

Results of the different calculations are presented in Table 6. The first row is the result for the Λ-N potential given in Chapter 3 and the N-N potential C", the second row is obtained for a N-N potential made up to fit the ^{4}He size ($\langle r^2\rangle^{1/2}$ = 1.70 fm), while the last row again uses the size fitting N-N potential, but a Λ-N force which fits the old (1966) Λ-N scattering data*. For the sake of comparison, the size parameter used in method 3) is adjusted

---

* $V_s = -81.5\ e^{-r^2/1.4^2} + 87.0\ e^{-r^2/1.125^2}$

$V_t = -191.5\ e^{-r^2/1.4^2} + 196.5\ e^{-r^2/1.3^2}$

TABLE 6

Λ binding energy of ${}^{5}_{\Lambda}$He obtained from different models

Scattering data fitted	Calculated rms radius of ^{4}He (in fm)	$B_\Lambda({}^{5}_{\Lambda}\text{He})$ (in MeV)				Radial Compression from method 2
		Method 1	Method 2	Method 3		
1968	1.86	5.13	5.81	6.06		2%
				Gaussian	Yukawa	2.2%
1968	1.71	6.34	7.01	7.25	7.27	
1966	1.71	5.03	5.78	6.01	6.04	3%

so as to give a rms radius equal to that obtained by method 2). Comparing the first and second rows shows that a $\sim$ 10% difference in the rms radius causes a change of 1.20 MeV in the Λ binding energy. This quantity will be used as a size correction for the other B_Λ ($^5_\Lambda$He) calculation.

Out of the three methods outlined above, method 2) is supposed to be the most precise. Method 3) assumes that the α-particle remains rigid when the Λ is added, and the Λ binding energy obtained is the largest. This larger B_Λ value also appears when the rigid α model result is compared with the Hartree-Fock calculation[22,37]. The Λ binding energy from method 1) is $\sim$ 1 MeV less than the others, thus showing the importance of a correlated wave function for ^{4}He.

The compression of the core due to the addition of the Λ is small $\sim$ 2% which indicates that the α core is almost unchanged, and explains why the B_Λ from methods 2) and 3) are close to each other. (Appendix 2).

The last column of Table 6 is the binding energy calculated with a cut-off Yukawa potential given by Bhaduri, Nogami and Van Dijk[23]. The Gaussian and Yukawa results are very close to each other which indicates that the Λ binding is shape independent as pointed out by Herndon and Tang[17].

The effects of the various corrections mentioned

in Chapter 3 are tabulated in Table 7. The odd state suppression is introduced by letting the Majorana exchange parameter m_Λ be different from zero. This effect is very small but non-zero, since the ls exchange matrix elements are not identical to the direct matrix element owing to that α_Λ and β_Λ are different from the nucleon α's and β's. Furthermore, the ${}^{5}_{\Lambda}$He ground state is found to have small admixtures of $(1s)^2(1p)^2$ nucleon configurations which leads to smaller exchange matrix elements. Nevertheless, the suppression is insignificant.

The coefficient C_Λ is taken to be 0.01,a magnitude obtained by fitting the "high" energy scattering (Fig. 3). The accuracy of C_Λ is subject to question, however, since the decrease in B_Λ is small $\sim$ 0.2 MeV, reasonable variation in C_Λ does not change B_Λ much.

The reduction due to the density dependence is rather considerable. The coefficient $C_{\Lambda 4}$, a measure of the strength of the density dependence, is determined by fitting the Λ binding energy in nuclear matter D_Λ*. $C_{\Lambda 4}$ is sensitive to the choice of m_Λ. 50% suppression (m_Λ = 0.25) and the

---

* D_Λ is calculated by first order perturbation.

$$D_\Lambda(C_{\Lambda 4}) = -\sum_{N=1}^{k_F} \langle \phi_N \phi_\Lambda | v_{N\Lambda} | \phi_N \phi_\Lambda \rangle$$

where $v_{N\Lambda}$ is given by (2.3), and ϕ_N, ϕ_Λ are plane-waves.

TABLE 7

Effects of momentum dependence, Majorana exchange and density dependence on the Λ binding energy

m_Λ	c_Λ	$c_{\Lambda 4}$	$B_\Lambda(^5He)$ (in MeV)
0.0	0.0	0.0	5.81
0.0	0.01	0.0	5.57
0.25	0.01	0.0	5.54
0.50	0.01	57.5	4.76
0.25	0.01	136.0	3.78

Serber force (m_Λ = 0.50) are chosen. Fig. 4 shows that a better result (closer to experimental value) is obtained for m_Λ = 0.25.

In order to compare these results with the calculations of other authors, a size correction is necessary. Here we just use the quantity 1.20 MeV obtained from Table 6 as a rough estimate for the size correction which is added to the corresponding B_Λ. For m_Λ = 0.25 and 0.5, B_Λ is 4.98 MeV and 5.96 MeV respectively which is compatible with the Hartree-Fock calculation with central and tensor forces[22/].

The density dependent force does reduce the Λ binding energy, but even a factor as large as 136 ρ^3 is not able to reproduce the experimental value. Some other mechanisms such as isospin suppression, ΛNN force, etc. have to be introduced.

CHAPTER 5

THE BINDING ENERGY OF THE p-SHELL HYPERNUCLEI

The problem of the overbinding of the Λ particle in ${}^{5}_{\Lambda}\mathrm{He}$ when using central forces that produce experimental cross-sections also exists for the p-shell hypernuclei. The purpose of this chapter is to discuss several mechanisms which reduce the Λ-binding energies in these hypernuclei.

The first two related mechanisms discussed here are the effects of the deformation of the nuclei and their corresponding hypernuclei, and the Majorana exchange component of the Λ-N force.

The theoretical consideration of deformation has been given in Chapter 2, and the effect of deformation on the nuclear binding energy has been discussed by Volkov[9]. Recently, the possibility of deformation was mentioned in the hypernuclear Hartree-Fock calculation of Bassichis and Gal[40], but no explicit change in the binding energy due the deformation effects was given.

Calculations for ${}^{7}\mathrm{Li}$, ${}^{8}_{\Lambda}\mathrm{Li}$; ${}^{8}\mathrm{Be}$, ${}^{9}_{\Lambda}\mathrm{Be}$; ${}^{10}\mathrm{B}$, ${}^{11}_{\Lambda}\mathrm{B}$ and ${}^{12}\mathrm{C}$, ${}^{13}_{\Lambda}\mathrm{C}$ are presented as examples. A variational and configuration mixing minimization of the binding energy is performed. All the possible Slater determinants for a given

nucleus are constructed from a set of single particle wave functions of a cylindrical harmonic oscillator (Appendix 1)

$$\Psi_M = \frac{1}{\sqrt{A!}} \sum_P (-1)^P P \prod_{i=1}^{A} \psi_{n_i m_i n_{zi}}(\sqrt{\alpha_i}\rho_i, \phi_i, \sqrt{\beta_i} z_i) \chi_{m_{s_i}} \tau_{m_{t_i}}, \quad (5.1)$$

where P is one of the A! permutation operators for A particles. $\chi_{m_{s_i}}$ and $\tau_{m_{t_i}}$ are spin and isospin functions, and four nucleons are assumed to fill the $N = 0$ shell, i.e. the "1s" shell; and the remaining $A-4$ nucleons fill the $N = 1$, the "1p" shell, so as to give the smallest total $M = \sum_{i=1}^{A} (m_i + m_{s_i})$; and $M_t = \sum_{i=1}^{A} m_{t_i}$ must be appropriate to the nucleus being studied. If all the α's and β's in the states (5.1) are the same, then the results of matrix diagonalization are essentially the same as a conventional shell model calculation except no single particle energies are assumed and all particles are involved in the Hamiltonian.

The general procedure is to assume that $\alpha_\nu = \beta_\nu$ (the ν represents n, m, n_z), for a given major shell N, and then minimize the energy which is obtained from diagonalization of a sub-matrix spanned by the most important determinants, by varying the different α's. These size parameters are then used in the full matrix diagonalization to give the results for the 'spherical' representation. A more general calculation is for $\alpha_\nu \neq \beta_\nu$ and minimizes the energy for all possible oscillator constants (ν=[0,0,0],[0,0,1],[0,±1,0])

i.e. 3 α's and 3 β's for the nucleus orbitals, and α_Λ and β_Λ for the Λ particle which is, as in the case of $^{5}_{\Lambda}$He, assumed to be in a [0,0,0] state. This defines the 'deformed' representation. Thus the variation includes up to 8 parameters and as high as 158 determinants in the case of $^{11}_{\Lambda}$B. The effect of varying the different size parameters is essentially equivalent to mixing a number of different major shells in a Hartree-Fock calculation and characteristically the variation leads, in deformed nuclei, to an energy gain of a few MeV as well as a doubling of the mass quadruple moments.

The Λ binding energies for the different cases are given in Table 8. In all cases it is noted that there is a total hypernucleus binding energy gain by allowing the representation to deform since this represents a more complete variation. However, the Λ binding energy decreases for the better 'deformed' representation. The absolute value of the Λ binding energies should be taken with caution since the N-N force does not give the correct nuclear size except in the case of ^{7}Li. It is noted that the Λ binding energies are always smaller for $m_\Lambda = 0.5$ as compared with $m_\Lambda = 0.0$, and difference can be as large as 3.36 MeV for $^{13}_{\Lambda}$C. Herndon and Tang[17] have estimated that $m_\Lambda \approx 0.2$ in their analysis of the s-shell hypernuclei. It is also found that ΔB_Λ is decreased by about $0.3 \sim 0.4$ MeV for $m_\Lambda = 0.5$ as compared to $m_\Lambda = 0.0$.

TABLE 8

Binding energies in MeV for 1p shell nuclei, hypernuclei and Λ particle in "spherical" and "deformed" representations

	m_Λ	Spherical representation			Deformed representation			ΔB_Λ
		$B(^{A}X)$	$B(^{A+1}_{\Lambda}X)$	B_Λ	$B(^{A}X)$	$B(^{A+1}_{\Lambda}X)$	B_Λ	
^{6}He	0.0	24.11	32.81	8.70	25.80	33.70	7.90	-0.80
	0.5	24.11	31.72	7.61	25.80	32.97	7.17	-0.44
^{7}Li	0.0	36.28	47.51	11.23	39.11	49.61	10.51	-0.73
	0.5	36.28	46.23	9.95	39.11	48.76	9.65	-0.30
^{8}Be	0.0	50.38	64.01	13.63	55.59	68.38	12.79	-0.84
	0.5	50.38	62.18	11.80	55.59	66.99	11.40	-0.40
^{10}B	0.0	60.45	77.33	16.88	62.62	78.87	16.25	-0.63
	0.5	60.45	75.15	14.70	62.62	76.99	14.37	-0.33
^{12}C	0.0	87.09	108.57	21.48	89.70	110.82	21.12	-0.36
	0.5	87.09	104.84	17.75	89.70	107.46	17.76	+0.01

The reasons for these effects are as follows: the nuclear system deforms primarily in order to minimize its total kinetic energy since the total potential energy is insensitive to reasonable deformation because of exchange effects (Chapter 2). However, the Λ particle is in a state [0,0,0] where kinetic energy cannot be minimized by deformation; and if $m_\Lambda = 0.0$, the maximum potential energy is obtained by maximizing the ΛN wave function overlaps. A compromise is reached at the expense of Λ and nucleon kinetic energy. The Λ orbital becomes deformed and the nucleon orbitals become less deformed. This compromise results in less Λ binding energy. The deformation is represented by Q_N the nuclear quadruple moment in Table 9. A decrease in Q_N (in absolute value) is seen when the Λ is added to the nucleus.

The effect of deformation on B_Λ is further studied by allowing various deformations for the ${}^{8}_{\Lambda}\mathrm{Li}$ hypernucleus (Table 10). Q_N is the quadruple moment given by (A3.5). ΔB_Λ increases with the nuclear quadruple moment which is a measure of deformation, i.e. the more deformed the nucleus, the larger the decrease in Λ binding energy with the deformed representation.

For $m_\Lambda = 0.5$ the total Λ-N interaction decreases since a Λ-N exchange interaction introduces exchange matrix element

TABLE 9

The quadrupole moments of the nuclear cores and the Λ particle

Core Nucleus	Q_N (in barns) No Λ present	with Λ	Q_Λ (in mb)
^{6}He	0.031	0.026	6.4
^{7}Li	0.129	0.116	15.2
^{8}Be	0.250	0.215	23.4
^{10}B	0.175	0.158	14.4
^{12}C	-0.193	-0.186	-14.1

Q_N is given by (A3.5)

$$Q_\Lambda = 2\langle z_\Lambda^2 \rangle - \langle \rho_\Lambda^2 \rangle$$

TABLE 10

Effect of deformation on the Λ binding energy of $^{8}_{\Lambda}$Li

Q_N (without Λ)	Q_N (with Λ)	ΔB_Λ (in MeV)
0.134	0.118	0.52
0.129	0.116	0.30
0.117	0.112	0.16

Q_N is the quadrupole moment of ^{7}Li calculated with a deformed representation, ΔB_Λ is the difference in binding energies calculated from a spherical and a deformed representation, i.e $\Delta B_\Lambda = B_\Lambda$ (spherical) - B_Λ (deformed)

contributions at the expense of direct matrix contributions to the potnetial energy and the lp exchange matrix elements are smaller than the corresponding direct matrix elements. This leads to decreased binding. However, in this case since $v(r)\ P^x$ can be considered in terms of an equivalent velocity-dependent potential (2.25), it can be shown that the exchange matrix elements favour deformation and consequently in the final compromise, ΔB_Λ is smaller in magnitude than for $m_\Lambda = 0.0$. This follows since the Λ orbital can deform with less loss of energy.

Both deformation and Majorana exchange effects reduce the Λ-binding energies. However, they alone are unable to give the experimental binding. A still further reduction can be obtained by including density-dependence in both the N-N potentials and Λ-N potentials.

An indirect reduction of the Λ binding energy results from the use of a 'realistic' phenomenological density dependent N-N force which has been quite successful in a number of nuclear structure applications[41,42,43,44].

The main difference between a density independent and a density dependent N-N force in a hypernuclear calculation is the difference in the compression of the core by the Λ particle. To examine the effect of compression on the binding energy B_Λ, the following procedure is adopted. A non-

density dependent force is chosen to be

$$v_{ij} = [-78.03\ e^{-(r/1.5)^2} + 82.8\ e^{-(r/\lambda_R)^2}][0.29+0.71\ P^x+0.2P^\sigma-0.05P^\tau] \quad (5.2)$$

where $\lambda_R = 0.76\ (1 - 0.496\ (k-0.7)^2)$ and k is the relative momentum This force is able to reproduce the average ^1S and ^3S nucleon-nucleon scattering data, but saturates nuclear matter at much too high a density. The binding energy of the nucleus is first minimized with respect to the oscillator constants. The core is now kept rigid by retaining the same set of α's and β's, and the 'best' value of the hypernuclear binding energy is obtained by varying only the α_Λ and β_Λ. This binding energy is compared with that from a complete minimization, i.e. by allowing variation of all the α's and β's as well as α_Λ and β_Λ. It is noted in Table 11 that when the core is allowed to deform, an increase in the Λ binding energy appears together with a compression of the nuclear core. Similar calculations with a density dependent potential lead to similar but smaller compression and Λ binding energy gains.

The change in rms radii of the core due to the presence of the Λ particle is given in Table 11. The radial compression for the force without density dependence is of the order of 8% , a magnitude not too far from the result quoted by Bassichis and Gal for the Tabakin potential. For a density dependent N-N force, the compression is hindered,

TABLE 11

Variation in Λ binding energies to core compression

Core Nucleus	N-N force	$B(^{A}X)$	$B_\Lambda(^{A+1}_{\Lambda}X)$		ΔB	$\langle r^2\rangle^{1/2}$		$\frac{\Delta\langle r^2\rangle^{1/2}}{\langle r^2\rangle^{1/2}}$
			Core is rigid	Core is compressed		Without Λ	Compressed core	
^{7}Li	5.2	33.76	13.10	13.54	0.44	2.20	2.02	8.2%
	C"	39.11	10.47	10.51	0.04	2.53	2.49	1.6%
^{8}Be	5.2	50.26	15.34	15.68	0.34	2.24	2.14	4.5%
	C"	55.59	12.78	12.79	0.01	2.63	2.59	1.52%
^{12}C	5.2	80.88	30.49	30.86	0.37	2.28	2.15	5.75%
	C"	89.70	21.07	21.12	0.05	2.69	2.63	2.20%

$\langle r^2\rangle^{1/2}$ is the rms radius of the nuclear core

$\Delta\langle r^2\rangle^{1/2}$ is the radial compression due to the addition of the Λ particle.

since the N-N potential becomes weaker as the density is increased and $\Delta\langle r^2\rangle^{\frac{1}{2}}/\langle r^2\rangle^{\frac{1}{2}}$ is reduced to about 2%. Since it is less favourable in this case for the Λ particle to compress the core in order to increase the potential overlap, there is some reduction of the Λ binding energy compared to other calculations.

In analogy with the deformation effect, the compression effect is reduced by an increase of the Majorana exchange component in the Λ-N potential. In order to study the relation between the Λ binding energy, the density dependence in the N-N force and the Majorana exchange, the non-density dependent force (5.3) is modified so as to give the same radius for ^{7}Li as for the density dependent force. B_Λ is calculated for both forces. In spite of the equality the calculated rms radii and the use of the same Λ-N force, B_Λ differs for the two cases. The Λ binding energy is reduced by the use of a density dependent N-N potential. However the difference in B_Λ for the two different N-N forces decreases as m_Λ increases. (Table 12).

The compression effect on the Λ binding energy can be understood by the following argument. The direct Λ-N potential matrix element is proportional to the overlap integral which varies roughly as the nuclear density ρ. Thus for a force independent of ρ, the potential energy would favour a higher density, resulting in the compression of the core

TABLE 12

Sensitivity of Λ binding energies and radial compression to variations in Majorana exchange component

N-N force	m_Λ	$\langle r^2\rangle^{1/2}$ with the Λ present	$\Delta\langle r^2\rangle^{1/2}/\langle r^2\rangle^{1/2}$	$B_\Lambda(^8_\Lambda\mathrm{Li})$	ΔB_Λ
ρ independent	0.0	2.38	5.92%	10.88	0.37
ρ dependent	0.0	2.49	1.58%	10.51	
ρ independent	0.25	2.41	4.75%	10.31	0.21
ρ dependent	0.25	2.491	1.54%	10.10	
ρ independent	0.50	2.415	4.52%	9.80	0.15
ρ dependent	0.50	2.493	1.47%	9.65	
ρ independent	0.75	2.420	4.35%	9.22	0.0
ρ dependent	0.75	2.494	1.43%	9.22	

$\langle r^2\rangle^{1/2}$ for ^{7}Li = 2.53 fm,

ΔB is the Λ binding difference due to density dependence in N-N force

so as to increase ρ even though this leads to some increased kinetic energy. However, if we include a density term in the N-N force, an increase in ρ weakens the nucleon potential which decreases the potential energy gain as the system is compressed. The increase in the kinetic energy remains the same. Hence, the effect of the density dependence in the N-N force is to reduce the desirability for compression of the core. The gain in the Λ binding energy is therefore reduced relative to the density independent N-N case.

The exchange matrix element has been shown to be smaller than the direct matrix element and to be velocity dependent. If the velocity dependent oscillatory term were ignored, the relative increase of the Λ-N matrix element overlap would be the same as for the direct matrix element. However, the kinetic energy (velocity) of the nucleons increases as the core is compressed. The oscillatory factor therefore plays a greater role and reduces the gain due to overlap. Thus the effect of compression on the total potential energy is reduced, and the decrease in B_Λ due to the use of a density dependent N-N force diminishes with the increase of m_Λ.

If a density dependence is included in the Λ-N potential, the Λ binding energy can be reduced significantly. As mentioned in Chapter 3, a density dependence can be used

to make the Λ-N interaction spin dependent. This is because the range for the repulsive term is different for the singlet and the triplet force (r_R = 0.85 fm for triplet, 0.7 fm for singlet). Hence, even if we have the same factor $C_{\Lambda 4}\rho^3$ multiplying the radial part of the singlet and triplet component, the weakening of the interaction is different. To illustrate this effect, the first order Λ-potential energy in nuclear matter is given below:

V(singlet)=26.368 MeV, V(triplet)=26.267 MeV for $C_{\Lambda 4}$ = 0.0

V(singlet)=21.893 MeV, V(triplet)=16.744 MeV for $C_{\Lambda 4}$ = 100.0

An attempt is made to reproduce the ratio V_s/V_t obtained from the binding energies of the hypernuclei by allowing density dependence only in the triplet component. Fig. 4 shows that to reach the 'experimental' value of D_Λ, $C_{\Lambda 4}$ has to be about 157 which gives V_t = 11.21 MeV. Since $C_{\Lambda 4}$ = 0 for the singlet interaction, V_s remains at 26.368 MeV. The ratio V_t/V_s = 42.6% is much closer to that obtained from the Λ binding energies of $^{5}_{\Lambda}$He and $^{3}_{\Lambda}$H.

For finite nuclei we again take $^{8}_{\Lambda}$Li as our example.

For a nucleon in a [0,0,0] state, the first order potential energies are

$V_s([0,0,0]\Lambda)$=3.654 MeV, $V_t([0,0,0]\Lambda)$=3.602 MeV, $C_{\Lambda 4}$ = 0.0

$V_s([0,0,0]\Lambda)$=3.227 MeV, $V_t([0,0,0]\Lambda)$=2.975 MeV, $C_{\Lambda 4}$ = 136.0

$V_s([0,0,0]\Lambda)$=3.220 MeV, $V_t([0,0,0]\Lambda)$=2.840 MeV, $C_{\Lambda 4}$ = 0 singlet, 157 triplet

for a nucleon in a [0,0,1] state,

$V_s([0,0,1]\Lambda)=2.024$ MeV, $V_t([0,0,1]\Lambda)=2.080$ MeV, $C_{\Lambda 4}=0.0$

$V_s([0,0,1)\Lambda)=1.569$ MeV, $V_t([0,0,1]\Lambda)=1.532$ MeV, $C_{\Lambda 4}=136.0$

$V_s([0,0,1]\Lambda)=1.645$ MeV, $V_t([0,0,1]\Lambda)=1.622$ MeV, $C_{\Lambda 4}=\begin{matrix}0 \text{ singlet}\\ 157 \text{ triplet}\end{matrix}$

It is noted that the effect is more prominent when the nucleon is in the "1s" [0,0,0] state. When the nucleon is in the "1p" [0,0,1] state, the difference $V_s - V_t$ is small. This is because the p-shell nucleons are at the nuclear surface where the effective density is small, so even with $C_{\Lambda 4} = 157$ in the triplet potential and $C_{\Lambda 4} = 0$ in the singlet potential the difference in the corresponding potential energy is only about ~ 0.02 MeV. However, there is a decrease in energy with a density dependent Λ-N force even if the nucleon is in the 1p state. This is due to the change in the equilibrium orbital size, due to the effect of all interactions, rather than the direct effect of the density weakening of the [0,0,0]Λ, [0,0,1]N matrix elements.

The above discussion is entirely based on the difference in the repulsive range for the singlet and triplet force. However, the choice is rather arbitrary, and there is no reason why the repulsive range should be longer in the triplet component of the Λ-N interaction. Therefore, this is just a possible explanation of the spin discrepancy, and no conclusive remarks can be made concerning the relation

between the spin dependence and the density dependent force.

Like in the case of ${}^{5}_{\Lambda}He$, the Λ binding energy depends upon simultaneous change in m_{Λ} and $C_{\Lambda 4}$. Table 13 lists the values of B_{Λ} for different m_{Λ}. A size correction should be made in cases when the rms radii differ from the experimental values. However, it is noted that even without the size correction, the discrepancy of overbinding still persists. It is also noted that even if the force is capable of giving the value of D_{Λ}, it is still too strong for finite hypernuclei.

TABLE 13

Effect of density dependence on Λ binding energies

Hypernucleus	$C_{\Lambda 4}=57.5, m_{\Lambda}=0.5$	$C_{\Lambda 4}=136.0, m_{\Lambda}=0.25$
${}^{8}_{\Lambda}\mathrm{Li}$	8.68	7.25
${}^{9}_{\Lambda}\mathrm{Li}$	11.04	9.41
${}^{9}_{\Lambda}\mathrm{Be}$	10.24	9.21
${}^{11}_{\Lambda}\mathrm{B}$	12.75	11.45
${}^{12}_{\Lambda}\mathrm{B}$	13.78	12.68
${}^{13}_{\Lambda}\mathrm{C}$	16.86	15.06

CHAPTER 6

THE EXCITED STATES

In spite of the existence of about fifteen established hypernuclear species, there are hardly any excited states identified experimentally. An investigation of the energy spectrum can be a useful tool in the study of the Λ-N interaction, especially with respect to the spin dependence of the Λ-N potential.

The excited states of hypernuclei and the corresponding core nuclei are obtained by constructing an appropriate set of states and diagonalizing the matrices of the Hamiltonians given by (2.10) and (2.1) respectively. The "deformed" representation, defined in a previous chapter, does not lead to eigen states in which the total angular momentum J is a good quantum number. In order to have a definite J, J projection must be performed on the deformed states which is both difficult and tedious. To avoid the necessity of using the projection approach, we use the "spherical" representation described in Chapter 5, i.e. we let $\alpha_\nu = \beta_\nu$ for $\nu = [0,0,0]$, $[0,\pm1,0]$ and $[0,0,1]$. A variational calculation is performed to obtain the best value of the ground state energy. The oscillator constants are now kept fixed for

the spectrum calculation. The largest diagonalization occurs for the Slater determinant representation having the lowest total value of M, the z component of the angular momentum. The ground state must be included in this representation. The energy level corresponding to this value of M is obtained by diagonalization. A new representation with M increased by one is constructed. An energy matrix diagonalization is performed with the new representation to get the corresponding spectrum. The process is repeated until the representation of the highest possible M is used. It is noted that all states of higher M are degenerate with those of lower M. This follows since we are now dealing with a spherical representation, and states of the same J but different M values are degenerate, i.e. the diagonalization is creating states of good J. The value of J for a particular state is therefore equal to the highest value of M for a degenerate set of states. A sample spectrum is now shown which illustrates the method

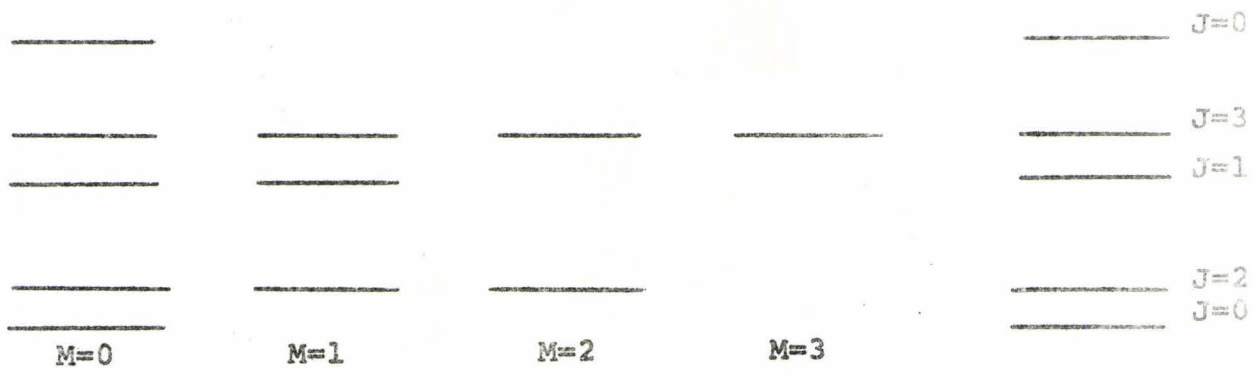

for determining the J values the energy eigenvalues.

The energy levels of a hypernucleus depend very much on the levels of the "core" nucleus. The spin dependence of the Λ-N interaction splits single states in the core nucleus into pairs of states in the hypernucleus. If the singlet component is stronger than the triplet one, the energy of the state associated with J_N-1/2, where J_N is the angular momentum value of the corresponding nuclear state, is lower than the corresponding J_N+1/2 state; and the splitting ΔE between the pair of states gives a measure of the difference between the singlet and triplet strength.

As mentioned before, the excitation energies of the hypernucleus depend sensitively on the spectrum of the core; and consequently, a calculation of the hypernuclear spectrum and the transition rates between levels is only meaningful if the N-N force is chosen to give a good fit to the experimental nuclear core spectrum.

^{6}Li and $^{7}_{\Lambda}$Li are taken as an example. The excited states of ^{6}Li are calculated with force C" given in Table 3 . The levels are shown in Fig. 7. They agree fairly well wuth the observed values. The spectrum of $^{7}_{\Lambda}$Li is calculated with the same N-N force and the Λ-N potential given in Chapter 3. It is noted that each of the levels of ^{6}Li splits into two, which are almost degenerate because the Λ-N singlet

and triplet interactions used for the calculation are not too different. A difference does show up in that the 1/2+ level is slightly lower than the 3/2+ level. If γ-rays between members of a pair could be detected experimentally, the γ-ray energy would give a measure of the spin dependence of the Λ-N interaction for the 1p-shell hypernuclei. However as yet no measurement has been made. Difficulty may result if the levels happen to be too close to each other.

The spectrum of ${}^{7}_{\Lambda}$He is of interest because it possesses an isomeric state. The experimental determination of $B_\Lambda({}^{7}_{\Lambda}\text{He})$ exhibits a double-peak structure with $B_\Lambda = 5.1\pm0.4$ MeV and $B_\Lambda^* = 3.2\pm0.4$ MeV. Pniewsky and Danysz[52] interpreted the B_Λ^* as an energy associated with an isomeric state of ${}^{7}_{\Lambda}$He. This is the only established experimental data for an excited state of a hypernucleus. The difference in the two binding energies $B_\Lambda - B_\Lambda^* = 1.9$ MeV is about equal to the excitation energy of the 2^+ level in ^{6}He.

This isomeric state has been studied in detail by Dalitz and Gal[27], in connection with the ΛN force spin dependence, and they found that $\Delta = V_s - V_t$ has to be less than 0.25 MeV for the isomeric state to exist. The existence of the isomeric state requires that the electromagnetic transition rates between the levels (5/2+→3/2+, 5/2+→1/2+ or 3/2+→1/2+) are smaller than the weak interaction decay rate of the Λ particle. Thus ${}^{7}_{\Lambda}$He decays by either the meson or

some other weak decay instead of undergoing a γ-transition.

The electromagnetic transition probability per second from a state I to a state F is given by

$$T = \frac{2\pi}{\hbar}|\langle F|H_{int}|I\rangle|^2\rho_E \qquad (6.1)$$

where ρ_E is the number of final states per unit energy interval, and H_{int} is the interaction between the particles and the electromagnetic field. After simplication (6.1) is of the form,

$$T(\sigma\Lambda) = \frac{8\pi(\lambda+1)}{\lambda[(2\lambda+1)!!]^2}\ \frac{k^{2\lambda+1}}{\hbar}\ B(\sigma\lambda) \qquad (6.2)$$

where

$$B(\sigma\Lambda, J_i\rightarrow J_f) = (2J_i+1)^{-1} \sum_{M_i,M_f} |\langle f|O_{\lambda\mu}|i\rangle|^2. \qquad (6.3)$$

Details of the derivation can be found in most standard texts on nuclear physics. The main assumption made in the derivation is that kR<<1, where R is the nuclear radius and k is given by $|E_i-E_f| = \hbar\omega = ck\hbar$. σ in (6.2) stands for either magnetic or electric multipole transitions and λ is the angular moment of the γ ray emitted. The $O_{\lambda\mu}$ in (6.3) is either an electric or magnetic multipole operator. The electric multipole operator is given by

$$O_{\lambda\mu} = \sum_i [e_i r_i^\lambda Y_\Lambda^{\mu*} - ig_{s_i}\mu_o k(\Lambda+1)^{-1}\underset{\sim}{\sigma}_i\times\underset{\sim}{r}_i\cdot\mathrm{grad}(r^\Lambda Y_\Lambda^{\mu*})_i] \qquad (6.4)$$

and the magnetic multipole operator is given by

$$M_{\lambda\mu} = \mu_o \sum_i \left(g_{s_i} \underset{\sim}{s}_i + \frac{2}{\lambda+1} g_{\ell_i} \underset{\sim}{\ell}_i\right) \cdot \text{grad}\ (r^{\Lambda} Y_{\Lambda}^{\mu *})_i . \quad (6.5)$$

μ_o is the nuclear magneton, and the g's are the gyromagnetic ratios.

For a E2 transition, the first term of (6.4) is simply the quadrupole moment operator whose matrix elements are given by (A3.6) , the second term of $Q_{\lambda\mu}$ is of the same order of magntidue as that of $M_{\lambda+1}$ and is usually ignored. The operator $M_{\lambda\mu}$ for $\lambda=1$ is given by

$$M1 = \mu_o \sum_k \left(g_k^{(\ell)} m_k + g_k m_{s_k}\right) \quad (6.6)$$

where g_k = 5.5856 for a proton, and -3.8263 for a neutron,

$g_k^{(\ell)}$ = 1 for a proton, and 0.0 for a neutron.

(6.4) is valid for both nuclei and hypernuclei since the Λ is a neutral particle which does not interact with the electric field so as to give rise to γ-ray . However the Λ particle has a non-zero magnetic moment. Thus it plays a role in the magnetic multipole transition and (6.6) has to be modified by adding a term $g_\Lambda m_\Lambda$ to include the Λ moment, where g_Λ = -1.46±0.34 n.m.

It is noted that T is proportional to $k^{2\lambda+1} = \left(\frac{E_i - E_f}{\hbar c}\right)^{2\lambda+1}$, i.e. T(E2) varies as $(E_i-E_f)^5$ and T(M1) varies as $(E_i-E_f)^3$, where E_i and E_f are the energies of the appropriate initial and final states.

In order to determine the E2 transition probability of $^{7}_{\Lambda}$He it was felt necessary to consider the effects of core polarization. The representation therefore should include all $2\hbar\omega$ excitations of the core. However, in that case the size of the matrix to be diagonalized becomes tremendously large; and due to the incapability of our computer to diagonalize this matrix, we have limited the excitation to only 2-particle excitations to the 1p shell from the 1s shell, and ignored the excitations to the 2s1d shell. The representation now includes up to 158 states for M = 1/2. The energy matrix is then diagonalized for different total M representations, as discussed earlier, in order to obtain the eigen energy states, and wave functions with definite J. The E2 rates from the excited states 5/2+ and 3/2+ to the ground state are then found to be of the order of 10^{7} sec^{-1} which is much smaller than the hypernuclear decay rate of 0.40×10^{10} sec^{-1}. Furthermore, in the above calculation, we have ignored the recoil of the charged α-particle relative to the centre-of-mass of $^{7}_{\Lambda}$He. This recoil amount has an opposite effect compared to the core excitation as discussed by Dalitz and Gal[27] and the final result of T(E2) is therefore less than $\sim 10^{7}$.

Next, we consider the M1 transition. The transition from the 3/2+ state to the 1/2+ state is caused by the transition of the $^{6}_{\Lambda}$He core from the J=2 to the J=1 state, and

$T(3/2+\rightarrow 1/2+,M1)$ is found to be 0.896×10^{9} sec^{-1}. The $5/2+\rightarrow 3/2+$ transition is due to the spin flip of the Λ particle. $T(5/2+\rightarrow 3/2+,M1)$ is proportional to the cube of the energy difference between the two states, and is found to be 3.03×10^{8} sec^{-1}. Hence, with the Λ-N potential used in this thesis, i.e. a potential which fits the scattering data and includes the density dependence, the 5/2+ and 3/2+ states are isomeric, thus leading to no contradiction between the experimental scattering data and the experimentally detected ${}^{7}_{\Lambda}He$ isomeric state.

CHAPTER 7

THE THREE BODY ΛNN FORCE

The $\Lambda\Sigma\pi$ coupling should in principle lead to a three-body ΛNN force as well as the two-body ΛN force. The lowest order ΛNN potential is generated when two pions emitted by a Λ are absorbed by different neighbouring nucleons as shown in Fig. 1c. This pion-exchange potential has central and strong non-central components such as the tensor force. The three-body ΛNN force appears to be repulsive on the basis of meson theory calculations[51].

Effects of the ΛNN force on the binding energies of light hypernuclei, such as ${}^{5}_{\Lambda}\mathrm{He}$ and ${}^{3}_{\Lambda}\mathrm{H}$, have been discussed in the work of Bhaduri, Louseau and Nogami[51] and the effects of a three-body force in p-shell hypernuclei have been previously examined by Bodmer and Murphy[46]. It has been pointed out by Weitzner[47] that for a strong repulsive ΛNN force, the binding energies of light hypernuclei can be accounted for with an almost spin independent two-body potential. Gal[48] has also estimated that it is possible to obtain the experimental value for $B_{\Lambda}({}^{5}_{\Lambda}\mathrm{He})$ provided that the singlet and triplet ΛN forces have the same strength and a central repulsive three-body force is used. Furthermore,

he[49] has also suggested that a strong ΛNN force can be used to explain the exceptionally large binding energy difference for some pairs of p-shell hypernuclei, e.g. the negative values of $B_\Lambda(^{9}_{\Lambda}\mathrm{Be}) - B_\Lambda(^{8}_{\Lambda}\mathrm{Li})$ and $B_\Lambda(^{13}_{\Lambda}\mathrm{C}) - B_\Lambda(^{12}_{\Lambda}\mathrm{B})$.

A ΛNN potential can be written in general as

$$V_{\Lambda NN} = \sum_{i<j=1}^{A} v_{\Lambda ij}(r_\Lambda, r_i, r_j),$$

where i,j stand for the two nucleons.

A typical matrix element is given by

$$\sum_{i<j} \int \phi_\Lambda^*(r_\Lambda)\Psi_\alpha^*(r_1,\ldots,r_A)v_{\Lambda ij}(r_\Lambda,r_i,r_j)\phi_{\Lambda'}(r_\Lambda)\Psi_\beta(r_1,\ldots,r_A)$$

$$d^3r_\Lambda\, d^3r_1 \ldots d^3r_A \qquad (7.1)$$

where Ψ_α and Ψ_β are antisymmetric wave functions of the core nucleus and $\phi_\Lambda(r_\Lambda)$ is the Λ wave function which, if taken to be an harmonic oscillator wave function as before, will include the size parameters α_Λ and β_Λ.

Integrating (7.1) over r_Λ gives

$$\sum_{i<j} \int \Psi_\alpha^*(r_1,\ldots,r_A)\ \bar{v}_{ij}(r_i,r_j,\alpha_\Lambda,\beta_\Lambda)\Psi_\beta(r_1,\ldots,r_A)$$

$$d^3r_1 \ldots d^3r_A$$

which is simply a matrix element of a two-body nucleon-nucleon potential. Hence the effect of a ΛNN interaction in a shell model calculation is equivalent to the addition of a term to the N-N force.

Several general features of this effective two-body potential $\bar{v}_{ij}$ are as follows:

1) Since $V_{\Lambda NN}$ is repulsive, $\bar{v}_{ij}$ will also be repulsive and therefore, it tends to act against the compression of nucleus;

2) Besides depending on r_i, r_j, $\bar{v}_{ij}$ is also a function of α_Λ and β_Λ. Thus, in a variational calculation this effective potential has to be determined self-consistently;

3) Even if only the central component of the ΛNN force is considered $\bar{v}_{ij}$ is in general non-central.

To give a qualitative description of the three-body ΛNN potential we used a δ-function force of the form

$$v_{ij\Lambda} = v_{30}\delta(r_\Lambda - r_i)\delta(r - r_j)[(1-m_3)+m_3 P^x] \qquad (7.2)$$

where m_3 is a constant and P^x the space exchange operator. The exchange component is simply an effective term which sums up the terms like $(\sigma_i \cdot \sigma_j)(\tau_i \cdot \tau_j)$, $(\sigma_i \cdot \sigma_\Lambda)(\tau_i \cdot \tau_\Lambda)$ etc. The range of a ΛNN force should be between one-pion and two-pion exchange range, since the intermediate state energy is $m_\Sigma - m_\Lambda + m_\pi \sim 260$ MeV. Thus the choice of a δ-function force is just a matter of mathematical convenience and the results obtained should only be taken as qualitative.

An approximate effective one-body potential $\bar{u}_3(r_\Lambda)$ for the Λ particle can be derived from first order perturbation

theory which gives

$$\bar{u}_3(r_\Lambda) = \sum_{i<j}^{A} \int \phi_i^*(r_i)\ \phi_j^*(r_j) v_{\Lambda,i,j}\ \phi_i(r_i)\phi_j(r_j) d^3r_i d^3r_j \quad (7.3)$$

since $v_{\Lambda,i,j}$ has the form (7.2), (7.3) can be written as proportional to $\sum_{i<j}^{A} \rho_i(r)\ \rho_j(r)$, where ρ_i, ρ_j are the densities for particles in the states $\phi_i(\underset{\sim}{r}_i)$ and $\phi_j(\underset{\sim}{r}_j)$. $\bar{u}_3$ can therefore be approximated by a density dependent interaction.

A variational calculation as described in previous chapters has been performed with the ΛNN component in the hamiltonian, i.e.

$$H = \sum_i T_i - T_{CM} + \sum_{i<j} (v_{ij} + v_{\Lambda ij}) + \sum_i v_{\Lambda i}. \quad (7.4)$$

In order to compare the effect of the three-body force and the density dependence in the two-body interaction, the density dependent effect is eliminated by setting $C_{\Lambda 4}=0$. The Λ binding energies and the core radii of the hypernuclei are given in Table 14. The choice of v_{30} = 5.0 MeV is arbitrary and is just chosen to give a really weak ΛNN potential.

It is noted that the reduction of $B_\Lambda(^{A+1}_{\Lambda}X)$ corresponding to a relatively weak three-body potential is quite large. As mentioned earlier, the repulsive ΛNN force tends to push the nucleus out, resulting in smaller nucleon compression. This latter effect was also found by Gal in connection with his Coulomb interaction calculation[48].

TABLE 14

The effect of ΛNN force on Λ binding energies and rms radii

	$B(^{A+1}_{\Lambda}X)$		rms radii of the nuclear core when Λ is present	
	without ΛNN force	with ΛNN force	without ΛNN force	with ΛNN force
$^{8}_{\Lambda}Li$	10.51	8.08	2.49	2.492
$^{9}_{\Lambda}Be$	12.79	10.04	2.59	2.59
$^{12}_{\Lambda}B$	16.68	13.53	2.60	2.61
$^{13}_{\Lambda}C$	21.12	17.66	2.63	2.64

$v_{30} = 5.0$ MeV

Effect of ΛNN force on the Λ binding energy of ${}^{5}_{\Lambda}He$ is studied by employing the rigid α model which has been found as good or better for ${}^{5}_{\Lambda}He$ than the variational calculations we have used (Chapter 4). The average Λ potential due to the three-body force in first order is given by

$$\bar{u}_3(r_\Lambda) = 6 \int v_{ij\Lambda}(r_i, r_j, r_\Lambda)\rho(r_i)\rho(r_j)d^3r_i d^3r_j \quad (7.5)$$

where the factor 6 indicates that there are six possible ΛNN bonds. Using force (7.2) we have

$$\bar{u}_3(r_\Lambda) = 24\pi^2 v_{30} r_\Lambda{}^4 \rho^2(r_\Lambda) \quad (7.6)$$

which is added to the one-body potential (A2.9).

In order to reduce $B_\Lambda({}^{5}_{\Lambda}He)$ to about its experimental value, v_{30} is taken to be 15.0 MeV which leads to $B_\Lambda({}^{5}_{\Lambda}He)$ = 3.497 MeV by the rigid α model. This value of v_{30} is able to reduce the Λ binding energy of ${}^{8}_{\Lambda}Li$ and ${}^{13}_{\Lambda}C$ to about 4 MeV and 11 MeV respectively. However, owing to that a δ-function is too rough an approximation to the ΛNN force and the uncertainty in the strength of the potential to which the Λ binding energy is very sensitive, no quantitative conclusion can really be given.

Recently two-channel formalism for the ΛNN force has been studied in detail by Nogami and Satoh[50] and they have found this formalism rather successful in reproducing the Λ binding energy in nuclear matter. Unfortunately our variational

programme did not have the capability of including the two-channel formalism. However, it is believed that a variational calculation with a properly derived ΛNN force could lead to more conclusive remarks concerning the effects of the three-body force.

CHAPTER 8

CONCLUSION

This thesis reports various attempts which have been made to reduce the Λ binding energy for hypernuclei from ${}^{5}_{\Lambda}$He to ${}^{13}_{\Lambda}$C. The decrease due to different effects is given in Table 15. It has been found that a "deformed" representation and a density dependent N-N potential together are able to reduce the Λ-binding of the p-shell hypernuclei by ∿ 1.0 MeV. However, these effects do not play a significant role in ${}^{5}_{\Lambda}$He, which has a spherical equilibrium shape and a small core compression.

The effect of Majorana exchange, i. e. the relative p-state suppression is important for hypernuclei with larger A, e.g. ${}^{13}_{\Lambda}$C, since the number of relative p interactions increase rapidly for A>4. The effect on $B_{\Lambda}({}^{5}_{\Lambda}\text{He})$ is insignificant, i.e. $\lesssim$ 1% Λ binding energy reduction for $m_{\Lambda} = 0.5$. It was noted that a larger Majorana exchange component in the Λ-N force reduces the effect of both deformation and compression; and for $m_{\Lambda} = 0.5$ the decrease in the Λ binding energy due to these two effects is about half the value for $m_{\Lambda} = 0.0$. Nevertheless, it should be noted that whenever a N-N force which allows for high compression, e.g. 10% radial compression, is used with a spherical representation, a correction

TABLE 15

Summary of various effects on Λ binding energies

Hypernucleus	Reduction of Λ binding energy due to			
	Deformation	*Density dependence in N-N force	Space exchange component, m_Λ=0.25	Density dependence in Λ-N potential
$^{5}_{\Lambda}$He	0.0	0.0	0.03	1.76
$^{7}_{\Lambda}$He	0.8	0.37	0.36	2.05
$^{8}_{\Lambda}$Li	0.73	0.40	0.43	2.55
$^{9}_{\Lambda}$Be	0.84	0.33	0.70	2.92
$^{11}_{\Lambda}$B	0.63	0.32	0.99	3.25
$^{12}_{\Lambda}$B	0.60	0.31	1.21	3.52
$^{13}_{\Lambda}$C	0.36	0.32	1.68	4.02

*The numbers in this column are the difference in the Λ binding energy gain by core compression when density dependent and density independent N-N force is used.

of 0.5 to 1.0 MeV should be subtracted from the Λ binding energies.

The energy dependence of our Λ-N force, which might be required to fit Λ-N high energy scattered data, leads to an approximate 0.2 MeV decrease in the Λ binding energy. This result is highly qualitative due to the lack of high energy scattering data which could possibly determine the parameter involved.

Density dependence in the Λ-N potential would reduce the Λ binding energy by a considerable amount. The density dependent term $C_{\Lambda 4}\rho^3$ is rather phenomenological, and there is no obvious physical reason why it should be the same for both the 1s- and 1p-shell nuclei, or for the singlet and triplet interaction. However, the scarcity of experimental data does not justify the introduction of more parameters.

The three-body force has been thought to be more important for hypernuclei than for nuclei. The reason is that the ΛNN interaction has Σ in the intermediate state as shown in Fig. 1c and the energy difference $m_\Sigma - m_\Lambda$ is about 80 MeV, while in the three nucleons case, instead of Σ we have the nucleon in excited states giving an energy difference much larger than 80 MeV. It has been found that a relatively weak ΛNN interaction is able to reduce the Λ binding energy quite significantly; but unless the strength of the ΛNN potential is properly derived theoretically, the calculation

including the three-body force can only lead, at best, to qualitative results.

Apart from the three-body force, the theoretical Λ particle overbinding is only partially removed by the various effects we have investigated. The isospin suppression discussed in Chapter 4 seems to be a promising mechanism to remove the remaining discrepancies. However, very little basic theoretical work has been done on this effect and there was not enough time to include an investigation of the isospin suppression effect in this work.

The importance of the excited states has been mentioned repeatedly by Dalitz[53]. Unfortunately no such state has been identified (except for the probable isomeric state in the case of ${}^{7}_{\Lambda}\mathrm{He}$). However, our limited study of hypernuclear excited states indicates the possibility of further determining the singlet-triplet differences in the Λ-N potential. We have also shown, by explicit calculation, that our forces are consistent with the existence of a ${}^{7}_{\Lambda}\mathrm{He}$ isomeric excited state.

It is hoped that Λ-N scattering data for the intermediate and high energy regions can be determined experimentally. This, together with the identification of some hypernuclear excited states, would be very helpful in the further study of the Λ-N interaction and the Λ particle energy dilemma.

APPENDIX 1

THE SINGLE-PARTICLE REPRESENTATION FOR CYLINDRICAL SYMMETRY

The wave equation for the three-dimension harmonic oscillator, in cylindrical coordinate is

$$\frac{1}{\rho}\frac{\partial}{\partial\rho}\left(\rho\frac{\partial\psi}{\partial\rho}\right) + \frac{1}{\rho^2}\frac{\partial^2\psi}{\partial\phi^2} + \frac{\partial^2\psi}{\partial z^2} + \left(\frac{2M}{\hbar^2}E - \alpha^2\rho^2 - \beta^2 z^2\right)\psi = 0 \quad \text{(A1.1)}$$

where the oscillation constants α and β are defined to be

$$\alpha = M\omega/\hbar, \qquad \beta = M\omega_z/\hbar, \qquad \text{(A1.2)}$$

where ω and ω_z are the oscillator frequencies.

The solution of (A1.1) has been given by Copley and Volkov[38] and is of the form

$$\psi_{n,m,z}(\sqrt{\alpha}\rho,\phi,\sqrt{\beta}z) = N_{nmn_z}\, e^{im\phi}(\alpha^{\frac{1}{2}}\rho)^{|m|}\, L_n^{|m|}(\alpha\rho^2)\, e^{-\frac{1}{2}\alpha\rho^2}\, H_{n_z}(\beta^{\frac{1}{2}}z)\, e^{-\frac{1}{2}\beta z^2} \quad \text{(A1.3)}$$

where the normalization constant

$$N_{nmn_z} = \frac{1}{\sqrt{2\pi}}\left(\frac{\beta}{\pi}\right)^{1/4}\sqrt{\frac{1}{2^{n_z}n_z!}}\sqrt{\frac{2\alpha n!}{(n+|m|)!}},$$

$H_{n_z}(\beta^{\frac{1}{2}}z)$ is the Hermite polynomial and n_z can be any integer greater than or equal to zero, and $L_n^{|m|}$, the associated Laguerre polynomial, can be expressed as

$$L_n^{|m|} = \sum_{s=0}^{n} \mathcal{L}_{ns}^{|m|}(\alpha)\rho^s$$

where the expansion coefficient $\mathcal{L}_{ns}^{|m|}(\alpha)$ has the value

$$\mathcal{L}_{ns}^{|m|}(\alpha) = \frac{(n+|m|)!\,(-\alpha)^s}{(n-s)!\,(|m|+s)!\,s!},$$

n is any non-negative integer, and where m, the z-component of the orbital angular momentum, can be any integer positive or negative. (A1.3) will also be denoted by $[n,m,n_z]$.

The eigenvalue E associated with (A1.3) is

$$E_{nmn_z} = (2n+|m|+1)\hbar\omega + (n_z+\tfrac{1}{2})\hbar\omega_z. \qquad \text{(A1.4)}$$

Since only the absolute value of m enters the energy (A1.4) states for ± m are degenerate.

The quantum number N is defined as $N \equiv 2n+|m|+n_z$. The state [0,0,0] has $N = 0$, which for $\alpha=\beta$ is equivalent to the spherical 1s state. The states [0,±1,0] and [0,0,1] all have $N = 1$. They are equivalent to the 1p states when $\alpha=\beta$. Six states have $N = 2$. The [0,±1,1] and [0,±2,0] states are equivalent to 1d spherical states for $\alpha=\beta$ while appropriate linear combinations of [1,0,0] and [0,0,2] form the fifth 1d state and the degenerate 2s state. In general, the cylindrical representation can always be transformed to spherical representation by letting $\omega = \omega_z$, and using

the appropriate unitary transformation. The energy is then

$$E = (2n+ m +n_z+\frac{3}{2})\hbar\omega$$
$$= (N + \frac{3}{2})\hbar\omega.$$

N is just the usual principal quantum number for a three dimensional spherical harmonic oscillator. States with the same N are degenerate in the spherical, $\alpha=\beta$, limit.

It should be noted that even in this "spherical" representation, the different orbital density distributions are not the same in all directions (except for the [0,0,0] orbital) since $\bar{x}^2 = \bar{y}^2 = \frac{1}{2}\bar{\rho}^2 = \frac{1}{2}(2n+|m|+1)/\alpha$ and $\bar{z}^2 = (n_z+\frac{1}{2})/\beta$. The values $\bar{x},\bar{y},\bar{z}$ depend on the quantum numbers as well as the oscillator constants.

In Chapter 2 it is shown that a minimization of the kinetic energy generally favours a deformed representation and that the deformation d corresponding to the minimum kinetic energy is

$$d_{min} = \frac{2n_z+1}{2n+|m|+1}.$$

Each single particle state favours a prolate, spherical or oblate representation according to whether $d \gtreqless 1$. Relation between n,m,n_z, d_{min} and τ_{nmn_z}, a dimensionless quantity, defined to be

$$\tau_{nmn_z} = (2n+|m|+1)^{3/2}(2n_z+1)^{1/3}, \qquad \text{(A1.4)}$$

is shown below. Comparison of (A1.4) and (2.14),(2.15) shows that τ_{nmn_z} is a measure of the minimized expectation value of the kinetic energy.

N	n	$\|m\|$	n_z	d_{min}	τ_{nmn_z}
0	0	0	0	1	1
1	0	$\|\pm1\|$	0	$1/\sqrt{2}$	$\sqrt[3]{4}$
1	0	0	1	$\sqrt{3}$	$\sqrt[3]{3}$
2	1	0	0	$1/\sqrt{3}$	$\sqrt[3]{9}$
2	0	$\|\pm2\|$	0	$1/\sqrt{3}$	$\sqrt[3]{9}$
2	0	$\|\pm1\|$	1	$\sqrt{3/2}$	$\sqrt[3]{12}$
2	0	0	2	$\sqrt{5}$	$\sqrt[3]{5}$

Kinetic energy minimization alone requires [0,0,0] to remain spherical, while [0,0,1] and [0,±1,0] lead to prolate and oblate representation deformation respectively. Kinetic energy minimization for states with N=2 also lead to different representation deformations as shown above.

APPENDIX 2

THE RIGID α MODEL

The rigid α model was first suggested by Dalitz and Downs[45]. The assumption is that the ^{4}He core is not affected by the addition of the Λ particle. It is noted that the rigid α model can be derived from the variational principle.

The binding energy of the 5-body system $^5_\Lambda$He is obtained by minimization of $(\Psi(^5_\Lambda\text{He})|H|\Psi(^5_\Lambda\text{He})>$ with the intrinsic Hamiltonian H given by

$$H = \sum_{i=1}^{4} T_i + T_\Lambda - T_{CM} + \sum_{i<j=1}^{4} v_{ij}\,(\underset{\sim}{r}_i-\underset{\sim}{r}_j) + \sum_{i=1}^{4}(\underset{\sim}{r}_i - \underset{\sim}{r}_\Lambda)$$

$$= \sum_{i=1}^{4} T_i + T_\Lambda - \frac{1}{2(4m+m_\Lambda)}(\underset{\sim}{P}_\alpha+\underset{\sim}{P}_\Lambda)^2 + \sum_{i<j=1}^{4} v_{ij}\,(\underset{\sim}{r}_i-\underset{\sim}{r}_j)$$

$$+ \sum_{i=1}^{4} v_{i\Lambda}\,(\underset{\sim}{r}_i-\underset{\sim}{r}_\Lambda) \qquad \text{(A2.1)}$$

where $\underset{\sim}{P}_\alpha = \sum_{i=1}^{4} \underset{\sim}{P}_i$ is the total momentum of ^{4}He, $\underset{\sim}{P}_\Lambda$ is the Λ momentum, and m, m_Λ are the nucleon and Λ mass respectively. To generate the rigid α equation, we write H as

$$H = H(^4\text{He}) + \frac{P^2}{2\mu} + \sum_{i=1}^{4} v_{i\Lambda}(\underset{\sim}{r}_i - \underset{\sim}{r}_\Lambda) \qquad \text{(A2.2)}$$

where $H(^4\text{He})$, the Hamiltonian of ^{4}He is equal to

$$H(^4He) = \sum_{i=1}^{4} T_i - \frac{P_\alpha^2}{2(4m)} + \sum_{i<j=1}^{4} v_{ij}\,(\underset{\sim}{r}_i - \underset{\sim}{r}_j) \quad . \qquad \text{(A2.3)}$$

$\underset{\sim}{P}$ is defined by

$$\underset{\sim}{P} = \frac{1}{4m+m_\Lambda}\,(4m\underset{\sim}{P}_\Lambda - m_\Lambda \underset{\sim}{P}_\alpha)$$

which is the moment conjugate to the coordinate $\underset{\sim}{x}_4$ defined below, and μ is the reduced mass of the Λ particle

$$\mu = {}^{4mm_\Lambda}/_{(4m+m_\Lambda)}.$$

A new coordinate system is introduced as shown in the diagram below, where c is the centre-of-mass of the ^{4}He and $\underset{\sim}{x}_1$, $\underset{\sim}{x}_2$, $\underset{\sim}{x}_3$ are the internal coordinates of ^{4}He. $H(^4He)$ is therefore only a function of $\underset{\sim}{x}_1$, $\underset{\sim}{x}_2$ and $\underset{\sim}{x}_3$.

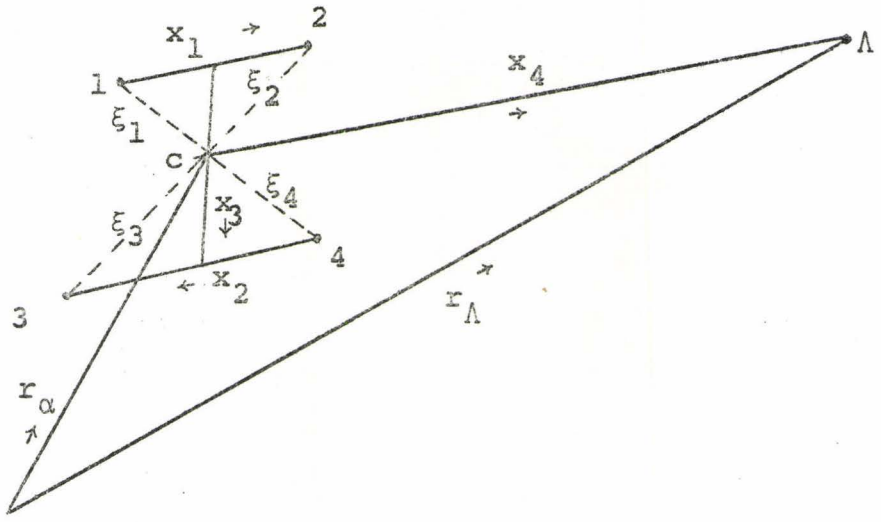

Furthermore the Λ-N interaction can be written as

$$v_{i\Lambda}(\underset{\sim}{r}_i-\underset{\sim}{r}_\Lambda) = v_{i\Lambda}(\underset{\sim}{x}_4-\underset{\sim}{\xi}_i),$$

where $\underset{\sim}{\xi}_i$ is some linear combination of $\underset{\sim}{x}_1$, $\underset{\sim}{x}_2$ and $\underset{\sim}{x}_3$.

The trial wave function is taken to be

$$\Psi = \chi(\underset{\sim}{x}_1,\underset{\sim}{x}_2,\underset{\sim}{x}_3)\phi_\Lambda(\underset{\sim}{x}_4) \tag{A2.4}$$

and

$$\langle\Psi|H|\Psi\rangle = E(^4\text{He}) + \langle\phi_\Lambda(\underset{\sim}{x}_4)|\frac{p^2}{2\mu} + \sum_{i=4}^{4} \int|\chi(\underset{\sim}{x}_1,\underset{\sim}{x}_2,\underset{\sim}{x}_3)|^2$$

$$v_{i\Lambda}(\underset{\sim}{x}_4-\underset{\sim}{\xi}_i)\ d^3\underset{\sim}{x}_1 d^3\underset{\sim}{x}_2 d^3\underset{\sim}{x}_3|\phi_\Lambda(\underset{\sim}{x}_4)\rangle \tag{A2.5}$$

where $E(^4\text{He}) = \langle\chi|H(^4\text{He})|\chi\rangle$ is the intrinsic energy of the α core.

(A2.5) can be written as

$$\langle\Psi|H|\Psi\rangle = E(^4\text{He}) + \langle\phi_\Lambda(\underset{\sim}{x}_4)|\frac{p^2}{2\mu} + \sum_{i=1}^{4} \int|\chi(\underset{\sim}{x}_1,\underset{\sim}{x}_2,\underset{\sim}{x}_3)|^2 v_{i\Lambda}(\underset{\sim}{x}_4-\underset{\sim}{R})$$

$$\delta(\underset{\sim}{R}-\underset{\sim}{\xi}_i)d^3\underset{\sim}{x}_1 d^3\underset{\sim}{x}_2 d^3\underset{\sim}{x}_3 d^3\underset{\sim}{R}|\phi_\Lambda(\underset{\sim}{x}_4)\rangle \tag{A2.6}$$

but the density of ^{4}He is given by

$$\rho(\underset{\sim}{R}) = \sum_{i=1}^{4} \int|\chi(\underset{\sim}{x}_1,\underset{\sim}{x}_2,\underset{\sim}{x}_3)|^2\delta(R-\underset{\sim}{\xi}_i)d^3\underset{\sim}{x}_1 d^3\underset{\sim}{x}_2 d^3\underset{\sim}{x}_3$$

which being substituted into (A2.6) leads to

$$\langle\Psi|H|\Psi\rangle = E(^4\text{He}) + \langle\phi_\Lambda(\underset{\sim}{x}_4)|\frac{p^2}{2\mu} + \int \rho(\underset{\sim}{R})\ v_{i\Lambda}(\underset{\sim}{x}_4-\underset{\sim}{R})d^3R|\phi_\Lambda(\underset{\sim}{x}_4)\rangle. \tag{A2.7}$$

The variational principle requires

$$\delta\langle\Psi|H|\Psi\rangle = 0$$

i.e. $\delta E(^4\text{He}) + \delta\langle\phi_\Lambda|\frac{P^2}{2\mu} + \int\rho(\underset{\sim}{R})v_{i\Lambda}(\underset{\sim}{x}_4-\underset{\sim}{R})d^3R|\phi_\Lambda\rangle = 0$.

However, because ^{4}He is assumed to be rigid, $\delta E(^4\text{He}) \equiv 0$,

and $\delta\langle\phi_\Lambda|\frac{P^2}{2\mu} + \int \rho(\underset{\sim}{R})\ v_{i\Lambda}(\underset{\sim}{x}_4-\underset{\sim}{R})d^3\underset{\sim}{R}|\phi_\Lambda\rangle = 0$ with the condition $\langle\phi_\Lambda|\phi_\Lambda\rangle = 1$ leads to the rigid α equation

$$[\frac{P^2}{2\mu} + v_\Lambda(x_4)]\phi_\Lambda = E_\Lambda\phi_\Lambda \qquad \text{(A2.8)}$$

where the one-body potential $v_\Lambda(x_4)$ is given by

$$v_\Lambda(\underset{\sim}{x}_4) = \int \rho(\underset{\sim}{R})\ v_{i\Lambda}(\underset{\sim}{x}_4-\underset{\sim}{R})d^3\underset{\sim}{R}.$$

Substituting (A2.8) into (A2.7) gives

$$E_\Lambda = E(^5_\Lambda\text{He}) - E(^4\text{He}),$$

$-E_\Lambda$ is therefore the Λ binding energy in $^5_\Lambda$He.

Although the rigid α model assumes the core remains unchanged, the fundamental derivation is variational in nature. The variation is concentrated on ϕ_Λ and if the core indeed does remain rigid the value for E_Λ should be good. The method also has the virtue that an experimental density $\rho(R)$ can be used in the calculation. Any improvement in the method, i.e. allowing additional variation in the ^{4}He wave function, should increase the Λ particle binding energy and therefore $-E_\Lambda$ represents a lower bound for the Λ particle binding energy.

The one-body potential v_Λ for the two-body Λ-N force (3.3) can be determined as follows.

The nuclear density is assumed to be Gaussian

$$\rho(r) = Ne^{-\alpha r^2} ,$$

where N the normalization constant is equal to $(\alpha/\pi)^{3/2}$. α is related to the rms radius with respect to the CM by

$$\langle r^2 \rangle = \int r^2 \rho \, d^3\underset{\sim}{r}$$

which gives $\langle r^2 \rangle = \frac{3}{2\alpha}$.

For a central potential of the form

$$v_{i\Lambda} = V_a e^{-k_A r^2} + V_r e^{-k_R r^2}$$

v_Λ can be solved analytically to give

$$v_\Lambda(r) = V_a p_A^{3/2} e^{-\frac{1}{2}k_A p_A r^2} + v_r p_R^{3/2} e^{-\frac{1}{2}k_R p_R r^2} \qquad \text{(A2.9)}$$

where $$p_A = \frac{\alpha}{\alpha+0.5k_A} \text{ and } p_R = \frac{\alpha}{\alpha+0.5k_R} .$$

If $v_{i\Lambda}$ is density dependent and has the form

$$v_{i\Lambda} = V_a e^{-k_A r^2} + V_r(1 + C_{\Lambda 4}(4\rho)^n) e^{-k_R r^2} ,$$

then the term

$$C_{\Lambda 4} \, 4^n \, (\tfrac{\alpha}{\pi})^{\frac{1}{2}(3n+3)} V_r \int e^{-(n+1)\alpha r'^2} e^{-\frac{1}{2}k_R(\underset{\sim}{r}-\underset{\sim}{r}')^2} d^3\underset{\sim}{r}' \qquad \text{(A2.10)}$$

should be added to (A2.9).

The volume integral can be obtained by integrating $v_\Lambda(r_\Lambda)$ over the whole volume. It is equal to

$$u = (2\pi)^{3/2} \left(\frac{V_a}{k_A^{3/2}} + \frac{V_r}{k_R^{3/2}}\right) \qquad \text{(A2.11)}$$

and if $v_{i\Lambda}$ is density-dependence, a term given by integrating (A2.10) over the volume should be added.

APPENDIX 3

NUCLEAR SIZE AND MOMENTS

The rms radius

The rms radius r_m with respect to the nuclear centre-of-mass is defined by

$$r_m^2 = \frac{1}{A}\langle\Psi| \sum_{i=1}^{A} r_i^2 - \frac{1}{A}\Big(\sum_{i=1}^{A} r_i\Big)^2 |\Psi\rangle \qquad \text{(A3.1)}$$

where $\Psi = \sum_{\alpha} c_\alpha |\alpha\rangle$ with $|\alpha\rangle$ as the determinantal wave function of the A-particle system. (A3.1) can be written as the appropriate sum of one-body and two-body matrix elements

$$r_m^2 = \frac{1}{A}\Big(1 - \frac{1}{A}\Big) \sum_{i=1}^{A} \sum_{\alpha} \sum_{\beta} c_\alpha^{\,i}\, c_\beta^{\,i} \langle\alpha|r_i^2|\beta\rangle$$

$$- \frac{1}{A}\cdot\frac{2}{A} \sum_{i\neq j=1}^{A} \sum_{\alpha} \sum_{\beta} \sum_{\gamma} \sum_{\delta} c_\alpha^{\,i}\, c_\gamma^{\,i}\, c_\beta^{\,j}\, c_\delta^{\,j} \langle\alpha\beta|\underset{\sim}{r}_i \cdot \underset{\sim}{r}_j|\gamma\delta - \delta\gamma\rangle .$$

For ^{4}He, the second term will vanish identically by parity selection rules, if 2 particle - 2 hole excitations into the 1p shell are ignored. For this case

$$r_m^2 = \Big(1 - \frac{1}{A}\Big)\langle r^2\rangle \qquad \text{(A3.2)}$$

where $$\langle r^2 \rangle = \frac{1}{A} \sum_{i=1}^{A} \sum_{\alpha} \sum_{\beta} c_\alpha^{\,i} \, c_\beta^{\,i} \langle \alpha | r^2 | \beta \rangle \ . \qquad \text{(A3.3)}$$

(A3.3) is what is usually quoted as the experimental value, i.e. $\langle r^2 \rangle^{\frac{1}{2}} = 1.71$ fm.

For a shell model or Hartree-Fock calculation, the value of $\langle r^2 \rangle$ should be fitted. For the rigid α model, where the nucleon density function is chosen with respect to the centre-of-mass of the α-particle, r_m should be used instead of $\langle r^2 \rangle^{\frac{1}{2}}$.

In terms of the single particle wave function ϕ,

$$\langle r^2 \rangle = \frac{1}{A} \sum_{\alpha} c_\alpha^{\,2} \langle \alpha | \sum_{i=1}^{A} r_i^{\,2} | \alpha \rangle$$

$$+ \frac{1}{A} \sum_{\alpha \neq \beta} c_\alpha \, c_\beta \langle \alpha | \sum_{i=1}^{A} r_i^{\,2} | \beta \rangle$$

$$= \frac{1}{A} \Big[\sum_{\alpha} c_\alpha^{\,2} \sum_{j=1}^{A} \langle \phi_{\alpha_j} | r^2 | \phi_{\alpha_j} \rangle$$

$$+ \ 2 \sum_{\alpha < \beta} (-1)^{n_{\beta_\ell \alpha_m}} \langle \phi_{\beta_\ell} | r^2 | \phi_{\alpha_m} \rangle \Big] \qquad \text{(A3.4)}$$

where $(-1)^{n_{\beta_\ell \alpha_m}}$ is a phase factor determined by the position of β_ℓ, α_m in the determinantal wave function.

The quadruple moment

We define the static quadruple moment $\langle Q \rangle$ to be

$$\langle Q \rangle = \langle \alpha | \sum_{i=1}^{Z} 3z_i^2 - r_i^2 | \beta \rangle$$

which by analogy to (A3.4) is given by

$$\langle Q \rangle = \sum_{\alpha} c_\alpha^2 \sum_{j=1}^{Z} \langle \phi_{\alpha_j} | 3z^2 - r^2 | \phi_{\alpha_j} \rangle$$

$$+ 2 \Sigma (-1)^{n_{\beta_\ell \alpha_m}} \langle \phi_{\beta_\ell} | 3z^2 - r^2 | \phi_{\alpha_m} \rangle \qquad \text{(A3.5)}$$

The quadruple moment for transition probability between different states Ψ_i and Ψ_f where

$$\Psi_i = \sum_{\alpha} c_\alpha |\alpha\rangle \quad , \quad \Psi_f = \sum_{\beta} c_\beta |\beta\rangle \ ,$$

is determined by the matrix element

$$\langle \Psi_f | Q | \Psi_i \rangle = \sum_{\alpha} \sum_{\beta} c_\alpha c_\beta \left[\sum_i \langle \phi_i | 3z^2 - r^2 | \phi_i \rangle \right.$$

$$\left. (-1)^{n_{\beta\alpha}} \langle \phi_\beta | 3z^2 - r^2 | \phi_\alpha \rangle \right] . \qquad \text{(A3.6)}$$

APPENDIX 4

THE CENTRE-OF-MASS CORRECTION

The many body wave function $\Psi_i(\underset{\sim}{r}_1, \underset{\sim}{r}_2, \ldots \underset{\sim}{r}_A)$ can be written as $\psi_i(\underset{\sim}{\zeta}_1, \underset{\sim}{\zeta}_2, \ldots \underset{\sim}{\zeta}_{A-1}, \underset{\sim}{R})$, where the $\underset{\sim}{\zeta}$'s are appropriate relative coordinates and $\underset{\sim}{R} = \frac{1}{A} \sum_i \underset{\sim}{r}_i$ is the CM coordinate.

If an appropriate set of harmonic oscillator single particle wave functions is used as basis function , it is always possible to perform an exact separation of the form

$$\Phi_\nu(\underset{\sim}{\zeta}_1, \underset{\sim}{\zeta}_2, \ldots, \underset{\sim}{\zeta}_{A-1})\ \Theta_N(R)$$

where Θ_N is a harmonic oscillator function and Φ_ν represents an intrinsic state of the system. Elliot and Skryme[39] have shown that for shell model states with closed shells and valence particles in only one major shell, $N \equiv n = 1$, $\ell=0$, $m=0$ (1s ground state) i.e. the CM state is always in the lowest possible state. However, if there are particle hole excitations, then we can, after diagonalization get $\Phi_{\nu_1}\Theta_{1s}$, $\Phi_{\nu_2}\Theta_{1s}$, ... $\Phi_{\nu_N}\Theta_{1s}$, $\Phi_{\nu_1}\Theta_{2s}$ and possible other states of the form $\Phi_{\nu_3}\Theta_{2s}$ etc. The latter states, e.g. $\Phi_{\nu_1}\Theta_{2s}$ are spurious and would show up as

either

$$\frac{}{} \; E_{\nu_3}$$

$$\frac{\Phi_{\nu_2}\,\Theta_{1s}}{} \; E_{\nu_2}$$

$$\frac{\Phi_{\nu_1}\,\Theta_{1s}}{} \; E_{\nu_1} \qquad \frac{\Phi_{\nu_2}\,\Theta_{2s}}{}$$

if T_{CM} is subtracted from Hamiltonian

or

$$\frac{}{} \qquad \frac{\Phi_{\nu_1}(a\Theta_{1s}-b\Theta_{1s})}{}$$

$$\frac{\Phi_{\nu_2}\,\Theta_{1s}}{}$$

$$\frac{\Phi_{\nu_1}(a\Theta_{1s}+b\Theta_{1s})}{} \qquad a^2 + b^2 = 1$$

if T_{CM} is not subtracted from Hamiltonian

The method for eliminating the spurious state is outlined below. The CM hamiltonian has the form $H_{CM}=T_{CM}+\frac{1}{2}M\omega^2R^2$, where M is the mass of the whole system. H_{CM}, multiplied by a relatively large constant factor c, is added to the intrinsic hamiltonian of the system. The hamiltonian now can be written as

$$H = \sum_i T_i - T_{CM} + \sum_{i<j} V_{ij} + c\,\{T_{CM} + \frac{1}{2} M\omega^2 R^2\},$$

The energies associated with cH_{CM} will be $c(N+\frac{3}{2})\hbar\omega$, which is to be added to the intrinsic energy. If c is large enough, say c = 50, the energy levels corresponding to different N states of the CM will be distinctly separated when the total representation is diagonalized, i.e.

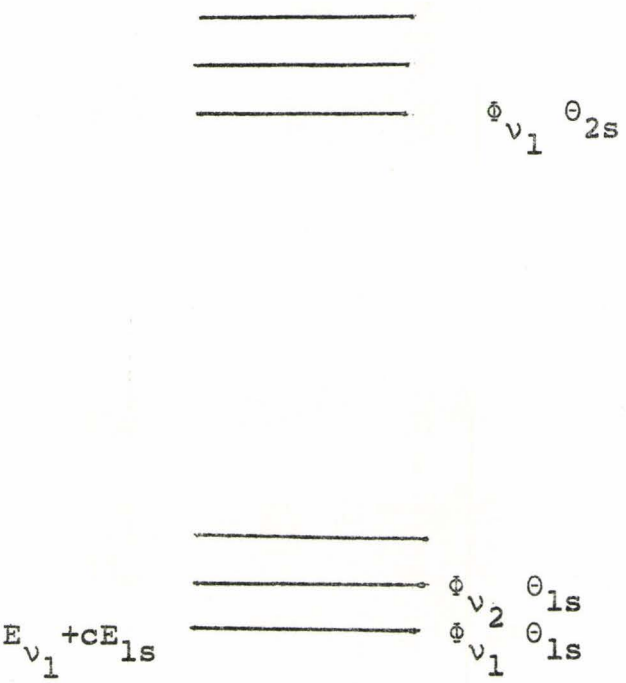

The spurious states can be discarded and the expectation value $\langle\Psi|cH_{CM}|\Psi\rangle$ can be calculated and subtracted from the energy spectrum of the non spurious spectrum so as to bring them to the correct energies. By using the great accuracy inherent in modern computers, the gap between spurious and non-spurious states can be made very large and the separation becomes very pure.

APPENDIX 5

THE THREE-BODY ΛNN POTENTIAL MATRIX ELEMENTS

The ΛNN force is assumed to have the form

$$V_{\Lambda NN}=\sum_{i<j}^{A} v_{\Lambda ij}(r_\Lambda,r_i,r_j)$$

$$=\sum_{i<j}^{A} v_{30}\ \delta(r_\Lambda-r_i)\,\delta(r_\Lambda-r_j)(1-m_3+m_3P^x) \qquad \text{(A5.1)}$$

where i,j are the two nucleons involved, P^x is the space exchange operator.

The general matrix element is written as

$$\langle\phi_\Lambda\ \Psi_{\{\alpha\}} \mid V_{\Lambda NN} \mid \phi_\Lambda,\ \Psi_{\{\beta\}}\rangle$$

where ϕ_Λ is the Λ wave function, and $\Psi_{\{\alpha\}}$, $\Psi_{\{\beta\}}$ are the determinental wave functions given by (2.8).

The diagonal matrix elements have $\{\alpha\} = \{\beta\}$ and therefore the diagonal matrix element is given by

$$\langle\phi_\Lambda\ \Psi_{\{\alpha\}} \mid V_{\Lambda NN} \mid \phi_\Lambda\ \Psi_{\{\alpha\}}\rangle$$

$$=\frac{1}{A!}\int\cdots\int\Big(\sum_P(-1)^P P\ \prod_{i=1}^{A}\phi_{\alpha_i}(r_i)\ \phi_\Lambda(r_\Lambda)\Big)^* V_{\Lambda NN}\Big(\sum_P(-1)^P P\ \prod_{i=1}^{A}\phi_{\alpha_i}(r_i)\phi_\Lambda(r_\Lambda)$$

$$d^3r_1 \ldots d^3r_A\, d^3r_\Lambda$$

$$= \int\ldots\int \left(\pi\ \phi_{\alpha_i}(r_i)\ \phi_\Lambda(r_\Lambda)\right)^*\ V_{\Lambda NN}\ \left(\sum_P (-1)^P\ P\ \prod_{i=1}^{A}\ \phi_{\alpha_i}(r_i)\right.$$

$$\left.\phi_\Lambda(r_\Lambda)\right) d^3r_1 \ldots d^3r_A\ d^3r_\Lambda$$

$$= \sum_{i<j=1}^{A} \iiint \phi_{\alpha_i}^*(r_i)\ \phi_{\alpha_j}^*(r_j)\ \phi_\Lambda^*(r_\Lambda)\ v_{30}$$

$$\delta(r_\Lambda - r_i)\,\delta(r_\Lambda - r_j)\,(1 - m_3 + m_3\ P^x)\,(\phi_{\alpha_i}(r_i)\ \phi_{\alpha_j}(r_j)$$

$$\left.\phi_\Lambda(r_\Lambda) - \phi_{\alpha_j}(r_i)\ \phi_{\alpha_i}(r_j)\ \phi_\Lambda(r_\Lambda)\right) d^3r_i\ d^3r_j\ d^3r_\Lambda$$

$$= v_{30} \sum_{i<j=1}^{A} \int \phi_{\alpha_i}^2(r_\Lambda)\ \phi_{\alpha_j}^2(r_\Lambda)\ \phi_\Lambda^2(r_\Lambda)\,(1 - \delta_K(m_{s_i} - m_{s_j})$$

$$\left.\delta(m_{t_i} - m_{t_j})\right) d^3r_\Lambda \qquad \text{(A5.2)}$$

where m_{s_i}, m_{s_j} and m_{t_i}, m_{t_j} are z-components of the spin and isospin of the i and j nucleons, and $\delta(x) = \begin{matrix} 1, & x = 0 \\ 0, & \text{otherwise} \end{matrix}$. The factor $1 - \delta_K(m_{s_i} - m_{s_j})\,\delta(m_{t_i} - m_{t_j}) = 0$, if $m_{s_i} = m_{s_j}$ and $m_{t_i} = m_{t_j}$. However, when the two nucleons are in the same spatial orbital, then the factor is always one.

Different off-diagonal matrix elements have to be treated separately.

For case 1 all the states in $\{\alpha\}$ are the same as those of $\{\beta\}$, but $\Lambda' \neq \Lambda$. Since the Λ particle is assumed to be in

the state [0,0,0], and it has T=0, the only possibility that $\Lambda \neq \Lambda'$ is when the z-component of the spin of the two states are different, i.e. $m_{s_\Lambda} \neq m_{s_{\Lambda'}}$. In this case $\langle \phi_\Lambda \Phi_{\{\alpha\}} | V_{\Lambda NN} | \phi_{\Lambda'} \Phi_{\{\alpha\}} \rangle = 0$, since we have assumed that the ΛNN force is spin dependent.

For case 2 $m_{s_\Lambda} = m_{s_{\Lambda'}}$ and all the states in $\{\alpha\}$ and $\{\beta\}$ match except for one state in each set. Let the different state in each set be α_i and α_i' respectively. The matrix element then has the form

$$v_{30} \sum_j \iiint \phi_\Lambda^*(r_\Lambda)\ \phi_{\alpha_i}^*(r_i)\ \phi_{\alpha_j}^*(r_j)(1-m_3+m_s P^x)$$

$$(\phi_\Lambda(r_\Lambda)\ \phi_{\alpha_i'}(r_i)\ \phi_{\alpha_j}(r_j) - \phi_\Lambda(r_\Lambda)\ \phi_{\alpha_j}(r_i)\ \phi_{\alpha_i'}(r_j))d^3r_\Lambda d^3r_i d^3r_j$$

$$= v_{30} \sum_j \int \phi_\Lambda^2(r_\Lambda)\ \phi_{\alpha_i}^*(r_\Lambda)\ \phi_{\alpha_i'}(r_\Lambda)\ \phi_{\alpha_j}^2(r_\Lambda)\ \delta_K(m_{s_{\alpha_i}} - m_{s_{\alpha_i'}})$$

$$\delta_K(m_{t_{\alpha_i}} - m_{t_{\alpha_i'}})[1 - \delta_K(m_{s_{\alpha_i}} - m_{s_{\alpha_j}})\ \delta_K(m_{t_{\alpha_i}} - m_{t_{\alpha_j}})]d^3r_\Lambda . \quad (A5.3)$$

For case 3 $m_{s_\Lambda} = m_{s_{\Lambda'}}$ and all the states in $\{\alpha\}$ and $\{\beta\}$ match except for two states in each set which we designate as $\alpha_i \neq \alpha_i'$ and $\beta_i \neq \beta_j'$. This class of matrix element can be written as

$$\iiint \phi_\Lambda^*(r_\Lambda)\ \phi_{\alpha_i}^*(r_i)\ \phi_{\alpha_j}^*(r_j)(1-m_3+m_3P^x)[\phi_\Lambda(r_\Lambda)\ \phi_{\alpha_i'}(r_i)$$

$$\phi_{\alpha_j'}(r_j) - \phi_\Lambda(r_\Lambda)\ \phi_{\alpha_j'}(r_j)\ \phi_{\alpha_i'}(r_j)\ d^3r_\Lambda\ d^3r_i\ d^3r_j$$

$$= \int \phi_\Lambda{}^2(r_\Lambda)\ \phi_{\alpha_i}{}^*(r_\Lambda)\ \phi_{\alpha_i'}(r_\Lambda)\ \phi_{\alpha_j}{}^*)(r_\Lambda)\phi_{\alpha_j}(r_\Lambda)$$

$$[\delta(m_{s_{\alpha_i}} - m_{s_{\alpha_i'}})\ \delta_K(m_{s_{\alpha_j}} - m_{s_{\alpha_j'}})\ \delta_K(m_{t_{\alpha_i}} - m_{t_{\alpha_i'}})$$

$$\delta_K(m_{t_{\alpha_j}} - m_{t_{\alpha_j'}}) - \delta(m_{s_i} - m_{s_{\alpha_j'}})\ \delta_K(m_{s_{\alpha_i'}} - m_{s_{\alpha_j}})$$

$$\delta_K(m_{t_{\alpha_i}} - m_{t_{\alpha_j'}})\ \delta_K(m_{t_{\alpha_i'}} - m_{t_{\alpha_j}})] \ . \qquad \text{(A5.4)}$$

If there are more than two states different from one another in the sets $\{\alpha\}$ and $\{\beta\}$, then the matrix element vanishes, since $V_{\Lambda NN}$, even though it is a three-body potential, contains only the two nucleon coordinates r_i and r_j.

REFERENCES

1. M. Danysz and J. Pniewski, Phil. Mag. 44, (1953) 348.
2. W. Gajewski, C. Mayeur, J. Sacton, P. Vilan, G. Wilquet, D. Harmsen, R. Levi Setti, M. Raymund, J. Zakrzewski, D. Stanley, D. H. Davis, E. R. Fletcher, J. E. Allen, V. A. Bull, A. P. Conway and P. V. March, Nucl. Phys. B1, (1967) 105.
3. D. H. Davis and J. Sacton, "Proceedings of the Second International Conference on High Energy Physics and Nuclear Structure", Rehovoth, 1967 (North-Holland Publishing Co., Amsterdam 1967).
4. G. Alexander, O. Benary, U. Karshon, A. Shapira, G. Yekutieli, R. Engelmann, H. Filthuth, A. Frieman and B. Schiby, Phys. Lett. 19, (1966) 715.
5. G. Alexander, U. Karshon, A. Shapira, G. Yekutieli, R. Engelmann, H. Filthuth and W. Lughofer, Phys. Rev. 173, (1968) 1452.
6. F. S. Crawford, M. Cresti, M. L. Good and F. T. Solmitz, Phys. Rev. Lett. 2, (1959) 174.
7. G. Alexander, Jared A. Anderson, Frank S. Crawford, Jr., William Laskar and Lester J. Lloyd, Phys. Rev. Lett. 7, (1961) 348.

8. B. Sechi - Zorn, B. Kehoe, J. Twitty and R. A. Burnstein, Phys. Rev. 175, (1968) 1735;
B. Sechi - Zorn, R. A. Burnstein, T. B. Day, B. Kehoe and G. A. Snow, Phys. Rev. Lett. 13, (1964) 282.

9. A. B. Volkov, Nucl. Phys. 74, (1965) 33;
A. B. Volkov, preprint.

10. P. Beillière, J. L. Gomez, A. Lloret, A. Rousset, K. Mykle-bost and J.M. Olsen, Phys. Lett. 12,(1964) 350.

11. L. Piekenbrack and F. Oppenheimer, Phys. Rev. Lett. 12 (1964) 625.

12. T. H. Groves, Phys. Rev. 129, (1963) 1372.

13. B. W. Downs and R.J.N. Phillips, Nuovo Cimento 33, (1964) 137.

14. A. Deloff, Nucl. Phys. B4, (1968) 585.

15. S. Ali. M. E.Gryperos and L. P. Kok, Phys. Lett. 24B, (1967) 543.

16. G. Alexander and U. Karshan, Proceedings of the Second International Conference on High Energy Physics and Nuclear Structure, Rehovath, 1967 (North-Holland Publishing Co., Amsterdam, 1967).

17. R. C. Herndon and Y. C. Tang, Phys. Rev. 153 (1967) 1091; Phys. Rev. 159, (1967) 853; Phys. Rev. 165 (1967) 1093.

18. J. Goldstone , Proc. Roy. Soc. (London) A239, (1957) 267.

19. H. A. Bethe, Phys. Rev. 167, (1968) 879.

20. S. Moszkowsky and B. Scott, Ann. of Phys. (N.Y.), 11, (1960) 65.

21. T. Kuo and G. Brown, Phys. Lett. 18, (1965) 54.

22. J. Law, M. R. Gunye and R. K. Bhaduri, preprint.

23. R. K. Bhaduri, Y. Nogami and W. Van Dijk, Phys. Rev. 155, (1967) 1671.

24. A. R. Bodmer and D. H. Rote, preprint, and references cited therein.

25. R. K. Bhaduri, Y. Nogami, P. H. Friesen and E. L. Tomusiak, Phys. Rev. Lett. 21, (1968) 1828.

26. R. K. Bhaduri and J. Law, preprint.

27. R. H. Dalitz and A. Gal, Nucl. Phys. B1, (1967) 1.

28. A. R. Bodmer, Proceedings of the International Conference on High Energy Physics and Nuclear Structure, Rehovoth, 1967 (North-Holland Publishing Co., Amsterdam 1967).

29. D. H. Wilkinson and M. E. Mafethe, Nucl. Phys. 85, (1966) 97.

30. R. Hofstadler, Rev. Mod. Phys. 28, (1956) 214.

31. M. R. Yearin, Proceedings of International Conference on Electromagnetic sizes of nuclei (Ottawa 1967).

32. M. M. Block et. al. Phys. Lett. 26B, (1968) 464.

33. S. Shastry and M. L. Rustgi, Phys. Lett. 25B, (1967) 391.

34. A. De-Shalit and J. D. Walecka, Phys. Rev. 147, (1966) 763.

35. B. R. Barrett, Phys. Rev. 154, (1967) 955.

36. C. Werntz and W. E. Meyerhof, Bull. Am. Phys. Soc. 12, (1967) 12.

37. B. F. Gibson, A. Goldberg and M. S. Weiss, Phys. Rev. 181, (1969) 1486.

38. L. A. Copley and A. B. Volkov, Nucl. Phys. 84 (1966) 417.

39. J. P. Elliot and T.H.R. Skyrme, Proc. Roy. Soc. A232, (1955) 561.

40. W.H. Bassichis and A. Gal, preprint.

41. M. R. Manning and A. B. Volkov, Phys. Lett. 26B, (1967) 60.

42. K. Lassey, M. R. Manning and A. B. Volkov, to be published.

43. D. H. Hughes and A. B. Volkov, to be published.

44. M. R. Manning, Thesis, McMaster University, unpublished.

45. R. H. Dalitz and B. W. Downs, Phys. Rev. 111, (1958) 967.

46. A. R. Bodmer and J. W. Murphy, Nucl. Phys. 64, (1965) 593.

47. H. Weitzner, Phys. Rev. 110, (1958) 593.

48. A. Gal, Phys. Rev. 152, (1966) 975.

49. A. Gal, Proceedings of the Second International Conference on High Energy Physics and Nuclear Structure, Rehovoth, 1967.(North-Holland Publishing Co., 1967).

50. Y. Nogami and E. Satoh, private communication.

51. R. K. Bhaduri, B. A. Loiseau and Y. Nogami, Ann. of Phys. 44, (1967) 57.

52. J. Priewski and M. Danysz, Phys. Lett. 1, (1962) 142.

53. R. H. Dalitz, "Nuclear Interactions of the Hyperons", (Oxd. University Press, 1965); Hypernuclear Physics, Lectures at the Varenna Summer School, 1966); Invited talk, International Conference on Hypernuclear Physics, Argonne National Laboratory, 1969.

FIGURE CAPTIONS

Figure 1(a) One-pion exchange graphs for the ΛN system, leading to the process $\Lambda N \rightarrow \Sigma N$

(b) Two-pion-exchange giving the lowest order contribution to the ΛN two-body potential

(c) Two-pion-exchange graph giving rise to a ΛNN three-body force

(d) K-meson-exchange graph leading to an exchange potential

Figure 2 The radial shape of the N-N potential for C" in Table 3; the difference between the two graphs showing the effect of the density dependence. A two-gaussian Λ-N potential is of the same shape but different strength and range.

Figure 3 The total elastic cross-section $\sigma_{\Lambda p}$ is plotted as a function of the CM kinetic energy. The theoretical curves are calculated with Λ-N potential given in Chapter 3 with different value of C_Λ.

Figure 4 The calculated well depth D_Λ and Λ binding energy $B_\Lambda(^5_\Lambda\text{He})$ are plotted as a function of $C_{\Lambda 4}$ for different Majorana exchange component in the Λ-N potential. Values of $B_\Lambda(^5_\Lambda\text{He})$ for $m_\Lambda = 0.25$ and $m_\Lambda = 0.5$ are almost identical, and the difference of 0.02 MeV cannot be shown distinctly in the graph.

Figure 5 A comparison of the experimental and calculated ^{4}He energy spectrum, the latter is obtained by using force C" in Table 3.

Figure 6 The ^{4}He binding energy is plotted as a function of its rms radius. The binding energy is obtained by a variational calculation with different "realistic" N-N forces which yield different equilibrium size.

Figure 7 Energy spectra of ^{6}Li and $^7_\Lambda$Li. Levels of energy higher than -26.5 MeV are not shown.

Figure 1

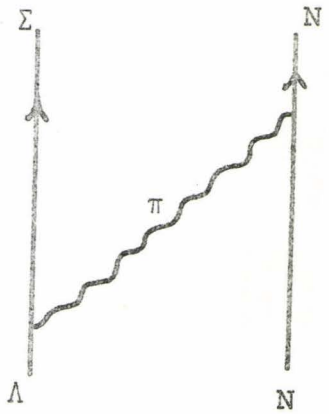

(a)

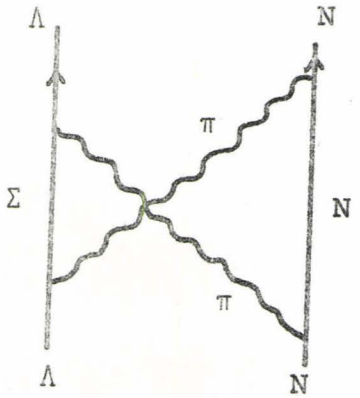

(b)

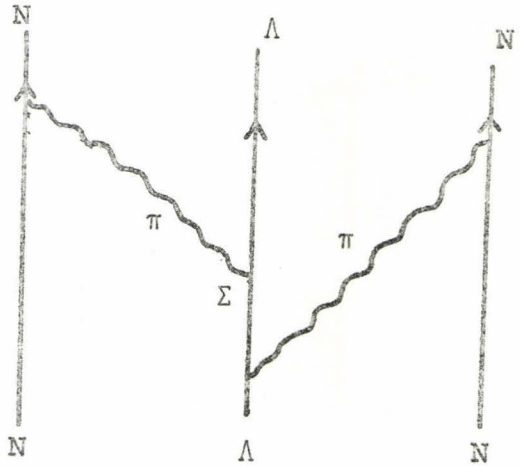

(c)

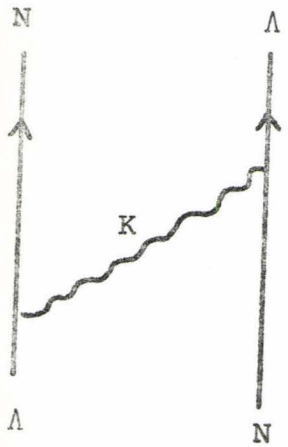

(d)

Figure 2

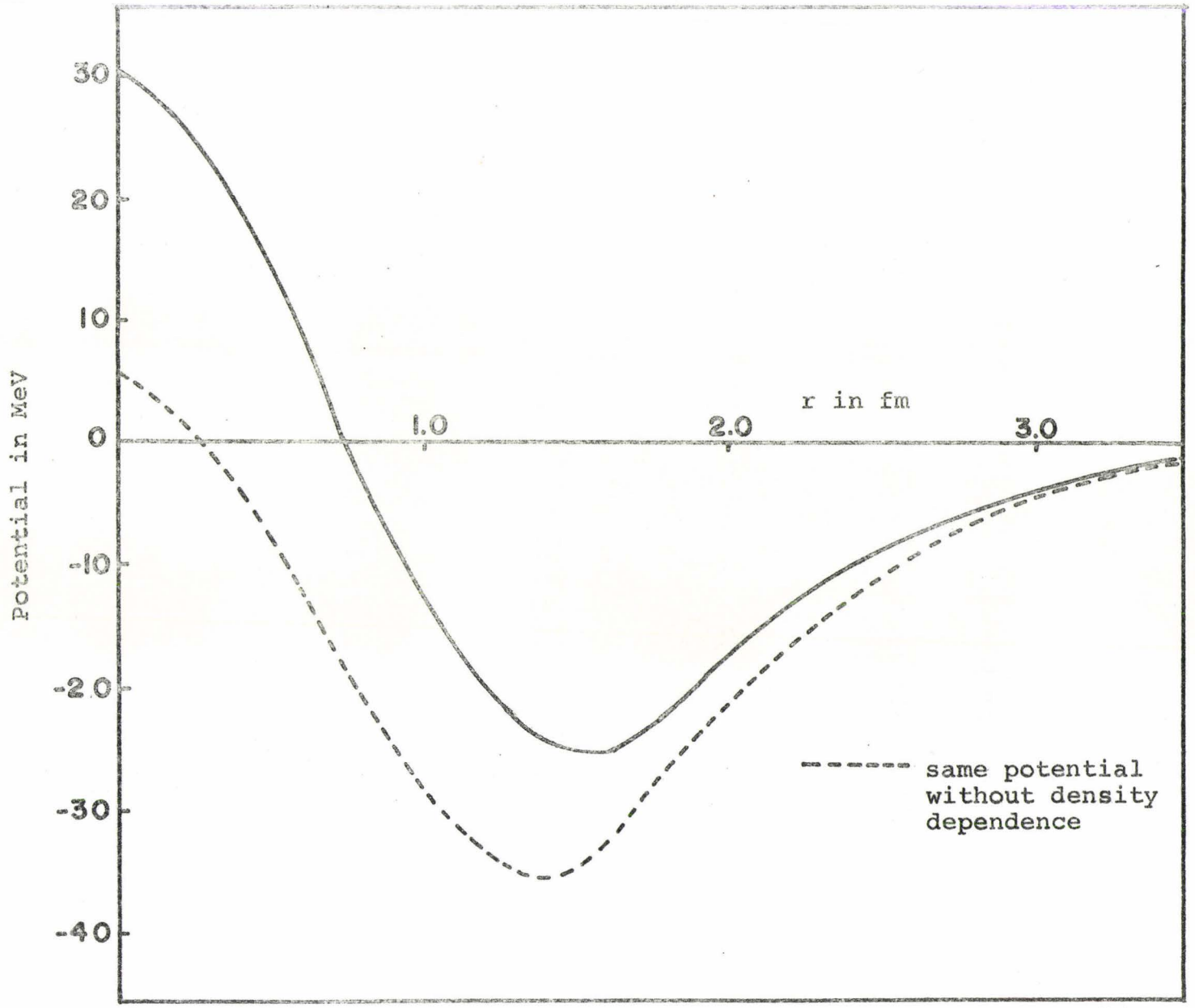
30
20
10
0
-10
-20
-30
-40
Potential in MeV
1.0
2.0
3.0
r in fm
same potential
without density
dependence

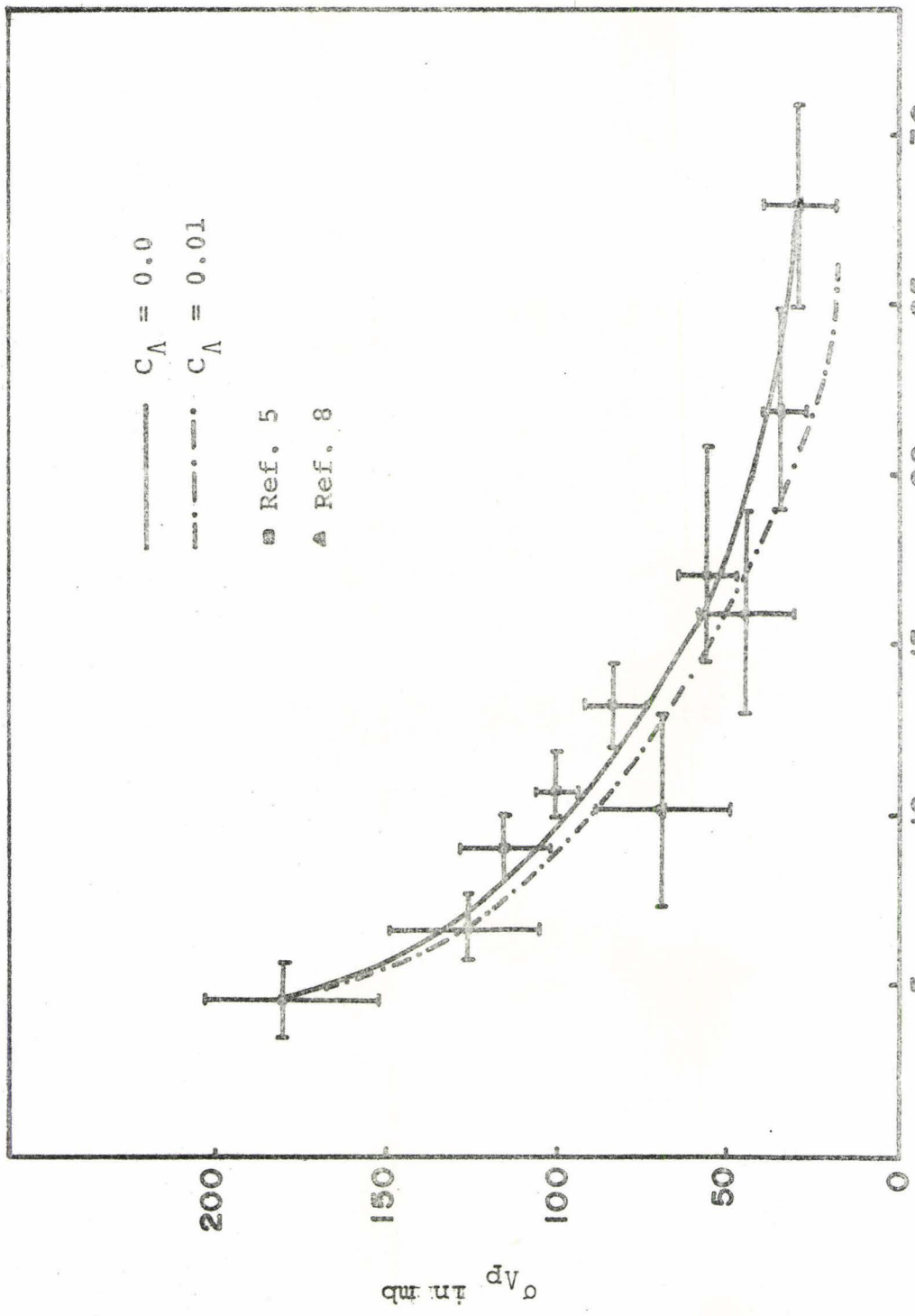
$C_\Lambda = 0.0$
$C_\Lambda = 0.01$
Ref. 5
Ref. 8
$\sigma_{\Lambda p}$ in mb
0
50
100
150
200
5
10
15
20
25
30
E_{CM} in MeV

Figure 3

Figure 4

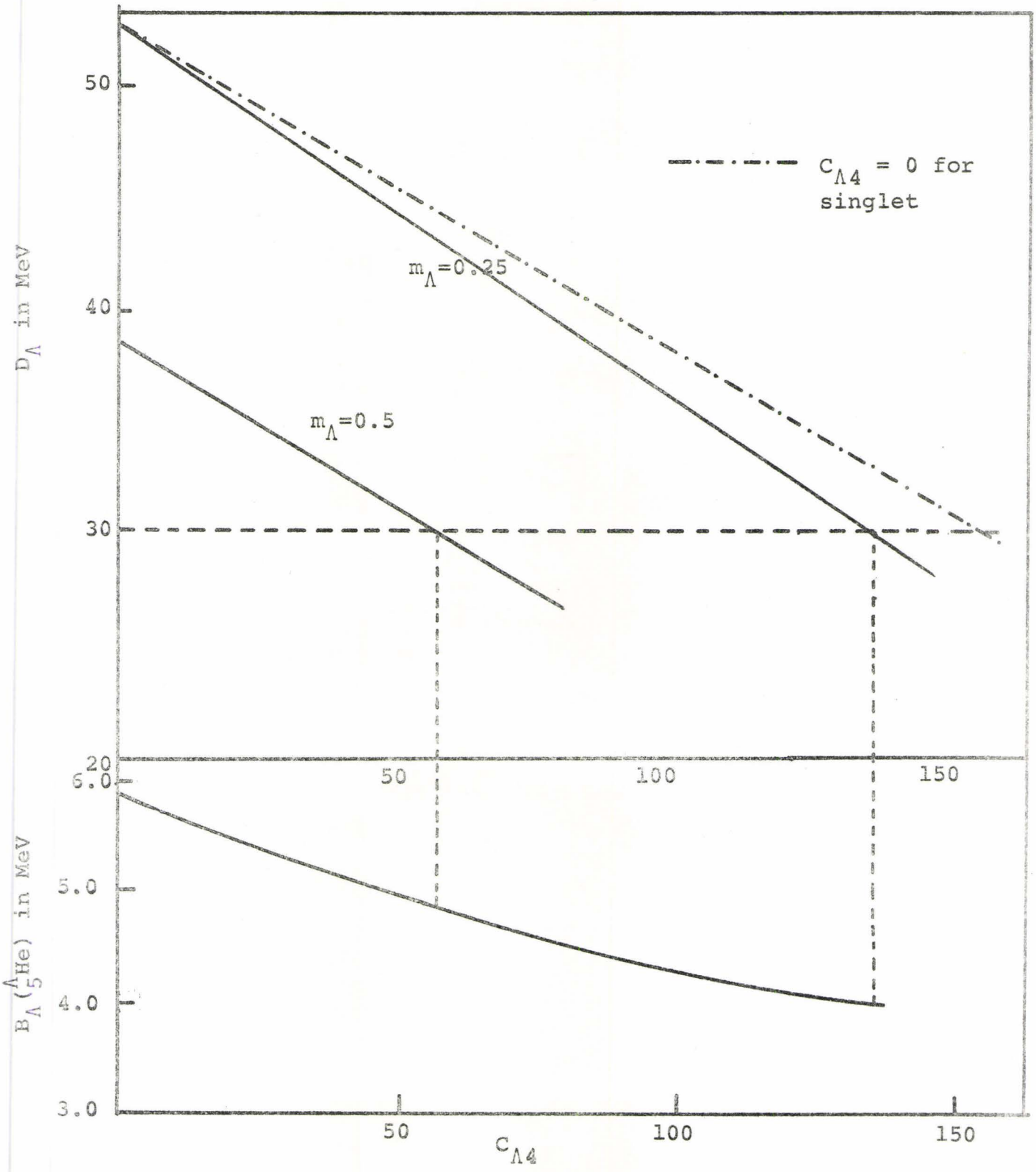
50
40
30
20
D_Λ in MeV
$C_{\Lambda 4}$ = 0 for singlet
m_Λ=0.25
m_Λ=0.5
50
100
150
6.0
5.0
4.0
3.0
$B_\Lambda(^{\Lambda}_{5}He)$ in MeV
50
100
150
$C_{\Lambda 4}$

Figure 5

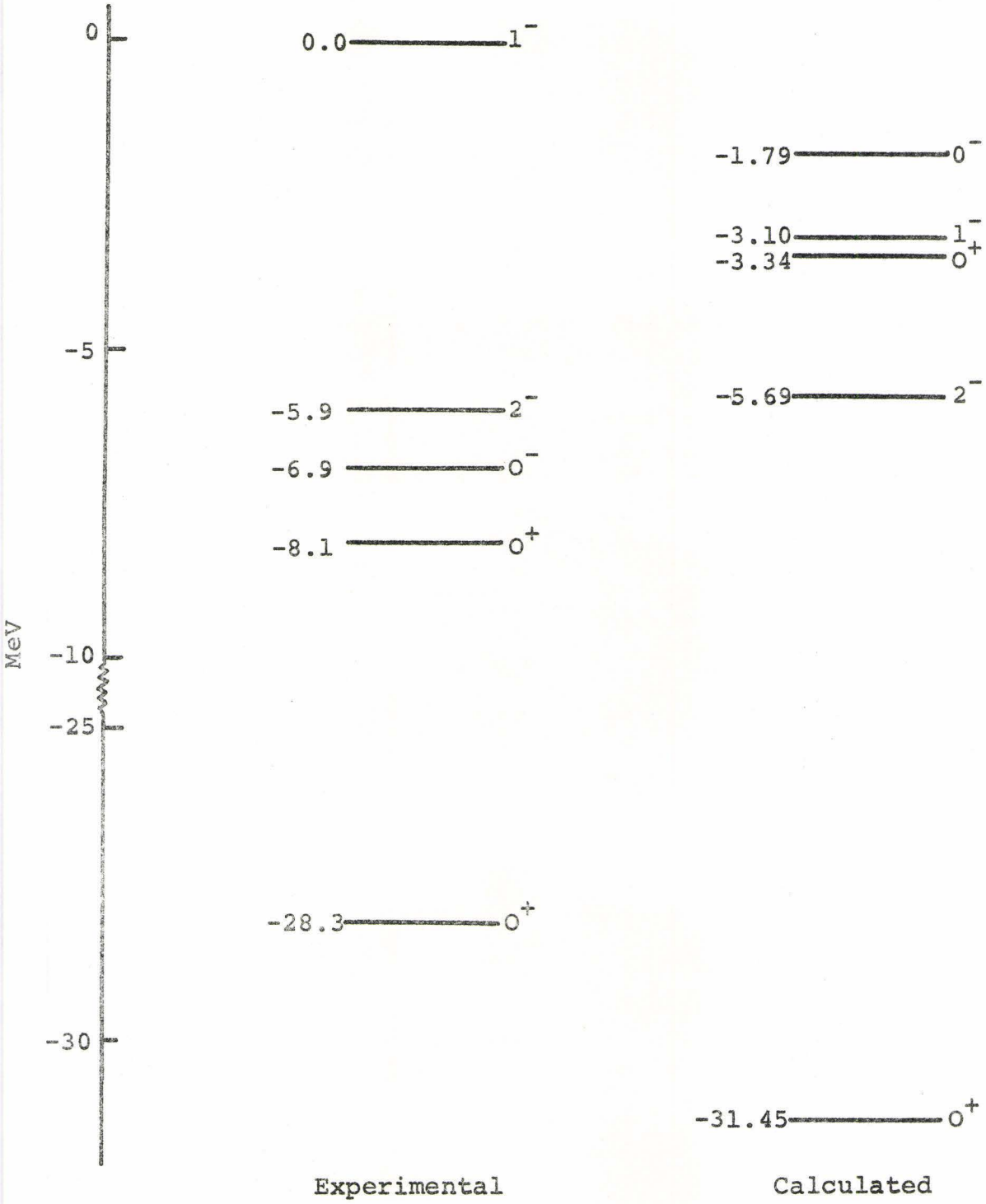
0
-5
-10
-25
-30
MeV
0.0 1⁻
-5.9 2⁻
-6.9 0⁻
-8.1 0⁺
-28.3 0⁺
-1.79 0⁻
-3.10 1⁻
-3.34 0⁺
-5.69 2⁻
-31.45 0⁺
Experimental
Calculated

Figure 6

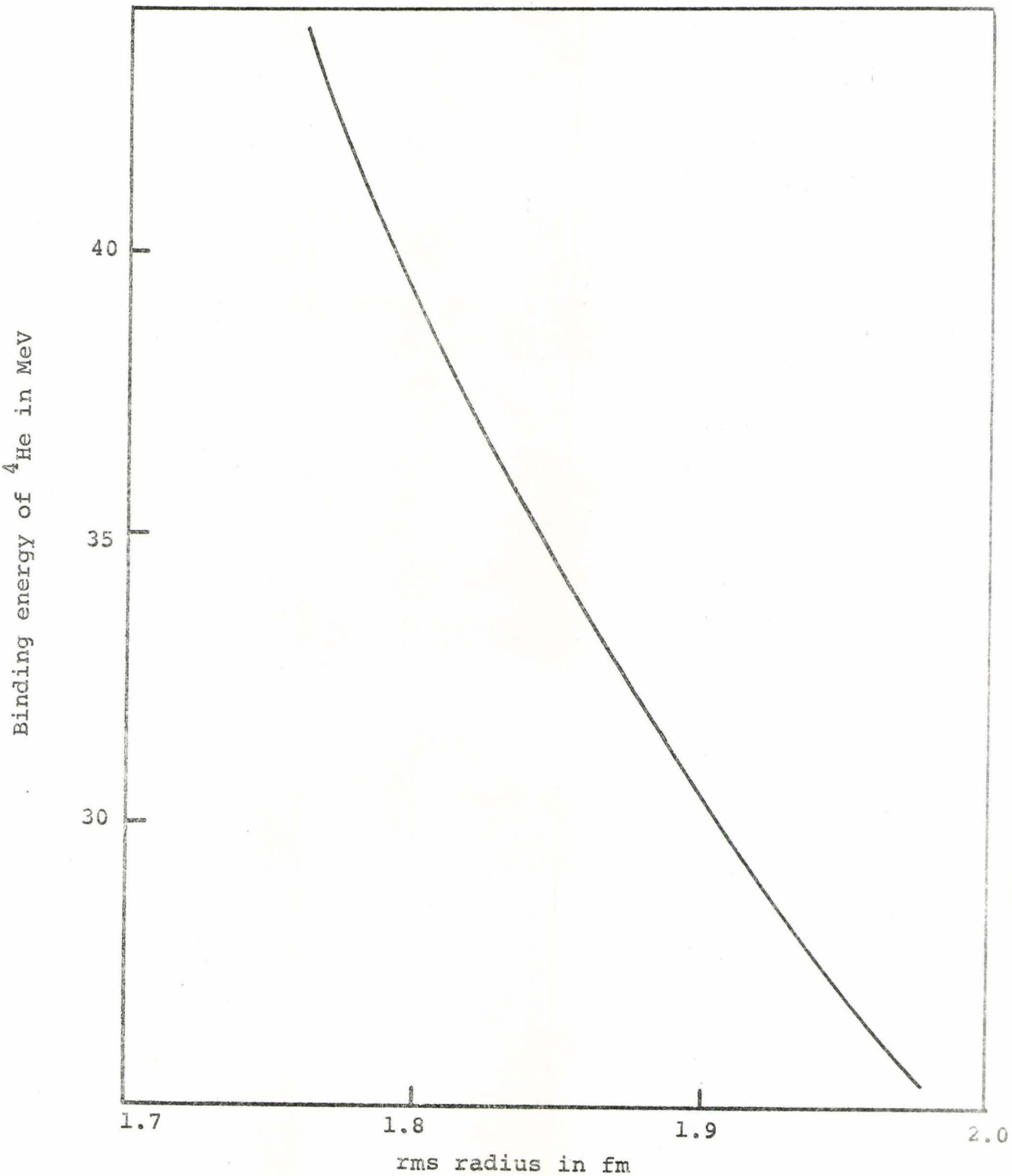
40
35
30
Binding energy of ^{4}He in MeV
1.7
1.8
1.9
2.0
rms radius in fm

Figure 7

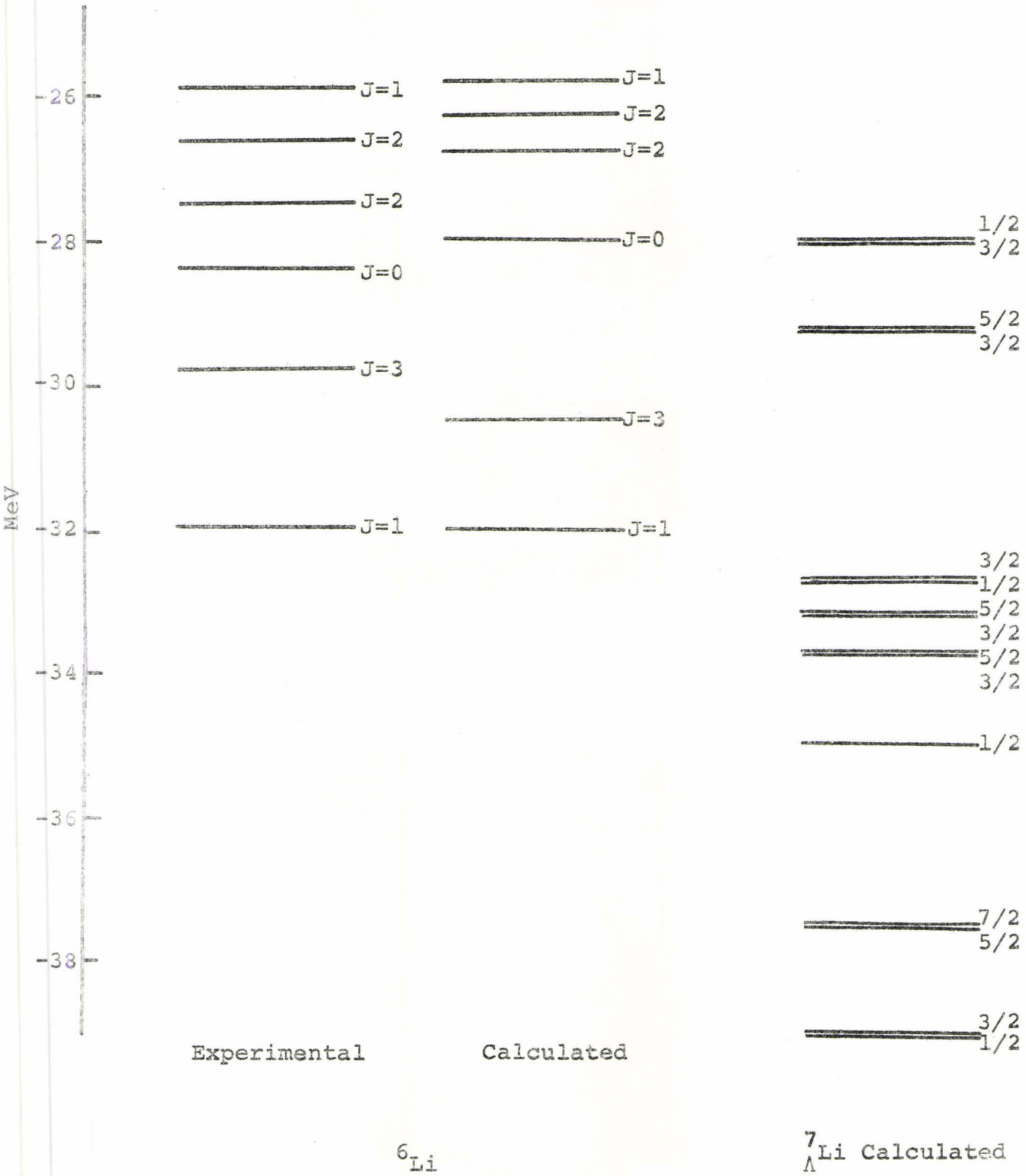
MeV
-26
-28
-30
-32
-34
-36
-38
J=1
J=2
J=2
J=0
J=3
J=1
J=1
J=2
J=2
J=0
J=3
J=1
1/2
3/2
5/2
3/2
3/2
1/2
5/2
3/2
5/2
3/2
1/2
7/2
5/2
3/2
1/2
Experimental
Calculated
$^{6}_{\Lambda}$Li
$^{7}_{\Lambda}$Li Calculated